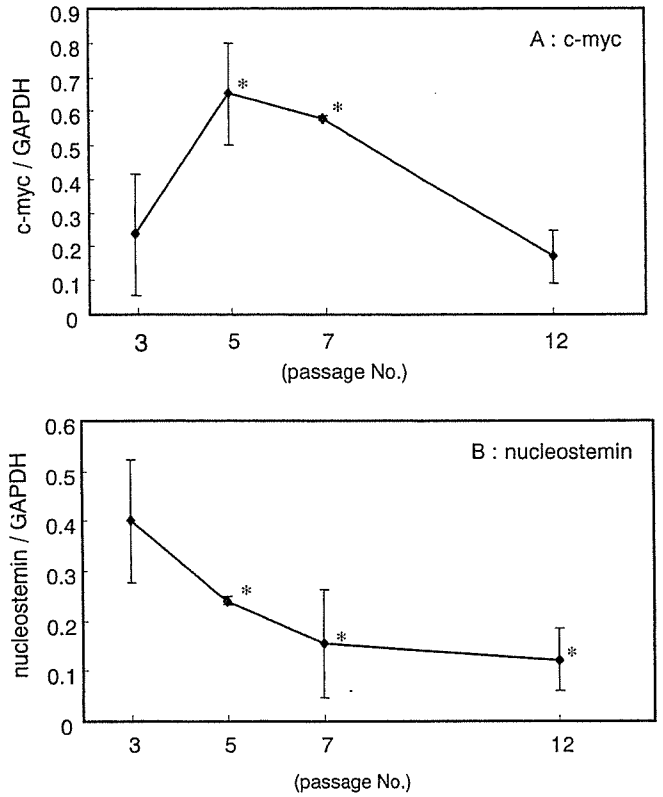


**Fig. 4.** Effect of in vitro culture length on the mRNA expressions of c-myc (**A**) and nucleostemin (**B**) in hMSCs. Expressions of the two genes relative to GAPDH in confluent cultures of hMSCs in the 3rd, 5th, 7th, and 12th passages were investigated by quantitative RT-PCR. Mean values with SDs from three independent experiments are presented. *Asterisks* denote statistically significant differences compared with the 3rd passage ($*P < 0.05$)

The mRNA expressions of TGFβs and TGFβ receptors in hMSCs of the fifth passage were compared with those of two kinds of cancer cells (HeLa S3 and HepG2) (Fig. 5). TGFβ1 mRNA levels in hMSCs and HepG2 cells were significantly higher than those in HeLa S3 cells (Fig. 5A). The mRNA expressions of TGFβ2, TGFβ3, TGFβRI, and TGFβRII in hMSCs were significantly higher than those in the cancer cells (HeLa S3 and HepG2) (Fig. 5B,C,D,E). TGFβRIII mRNA expression in hMSCs was significantly higher than that in HeLa S3, but lower than that in HepG2 (Fig. 5F). The expressions of several genes affecting cellular proliferation in all three cells were also investigated. The mRNA expressions of c-myc oncogene and nucleostemin in the cancer cells (HeLa S3 and HepG2) were significantly higher than those in hMSCs (Fig. 6A and B). Wnt-8B mRNA was expressed in the cancer cells (HeLa S3 and HepG2), but not in hMSCs (Fig. 6C). Wnt-8B mRNA was not expressed in any passage numbers of hMSCs (data not shown).

## Discussion

In this study, we investigated the changes of gene expression profiles during in vitro culture of hMSCs to evaluate their safety for use in clinical applications and tissue-engineered medical devices. First, the time dependency of the growth speed of hMSCs derived from bone marrow up to the 12th passage (at about 3 months) was investigated. The proliferation rate of hMSCs decreased by degrees during 3 months of in vitro culture (Fig. 1). No marked changes of hMSC morphology in 3 months of in vitro culture were

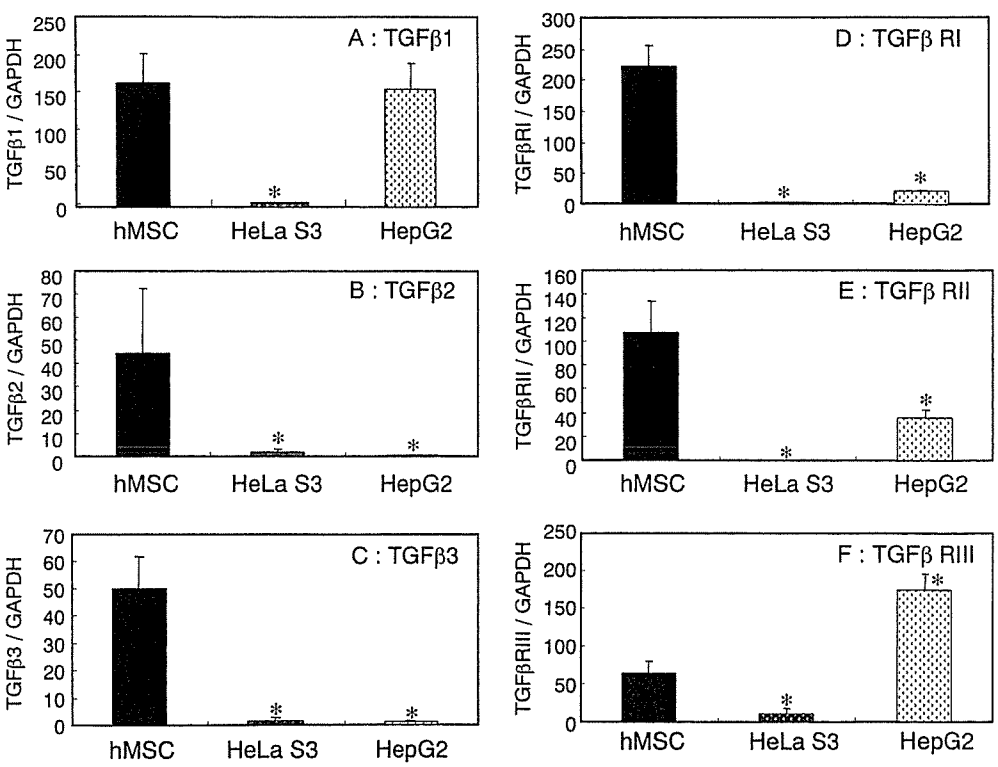


**Fig. 5.** mRNA expressions of TGFβ1 (**A**), TGFβ2 (**B**), TGFβ3 (**C**), TGFβRI (**D**), TGFβRII (**E**), and TGFβRIII (**F**) in hMSC, HeLa S3, and HepG2 cells. The expressions of the four genes relative to GAPDH in confluent cultures of hMSCs, HeLa S3, and HepG2 were investigated by quantitative RT-PCR. Mean values with SDs from three independent experiments are presented. *Asterisks* denote statistically significant differences from hMSCs ($*P < 0.05$)

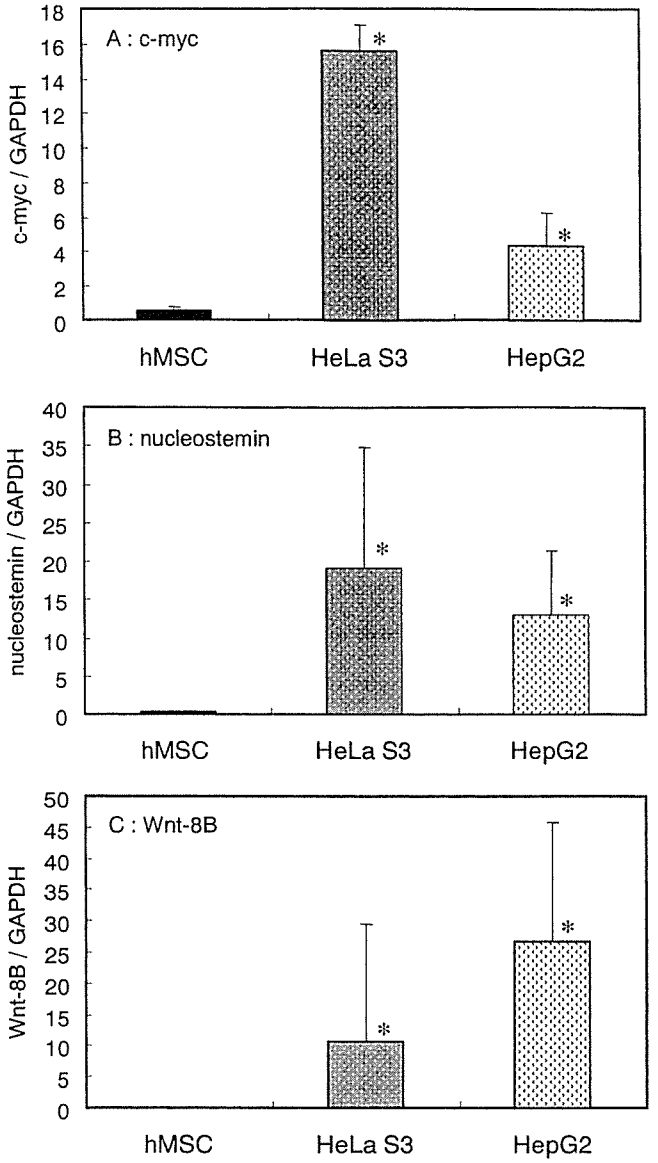


**Fig. 6.** mRNA expressions of c-myc (**A**), nucleostemin (**B**), and Wnt-8B (**C**) in hMSC, HeLa S3, and HepG2 cells. The expressions of the three genes relative to GAPDH in confluent cultures of hMSC, HeLa S3, and HepG2 cells were investigated by quantitative RT-PCR. Mean values with standard deviations from three independent experiments are presented. *Asterisks* denote statistically significant differences from hMSCs ($*P < 0.05$)

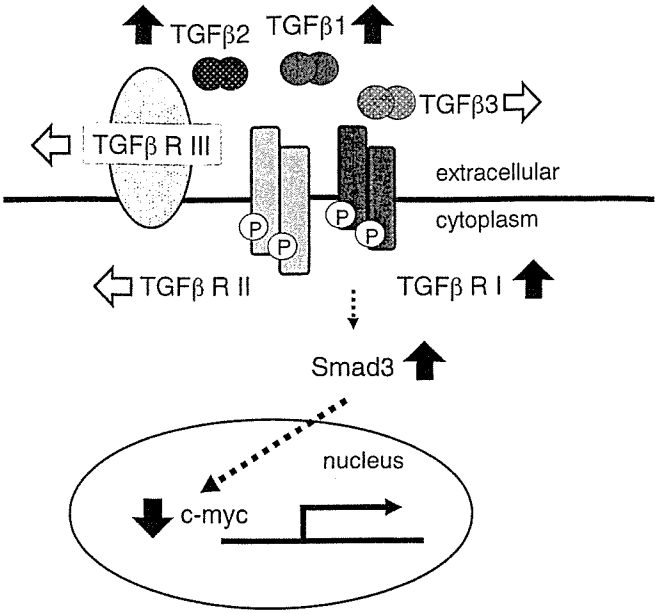


**Fig. 7.** Changes in the expressions of TGFβ signaling genes during hMSC in vitro culture for 3 months. The *dotted arrows* indicate the TGFβ signal pathway. *White arrows*, no changes; *black arrows*, up or down changes

observed. Several hMSCs derived from other donors' bone marrow did not undergo extraordinary proliferation either (data not shown). Adult stem cells have a self-renewal ability and undergo multilineage differentiation to maintain adult tissues.[9] In this study, however, hMSCs had more limited proliferative potential in in vitro culture. This phenomenon in hMSCs derived from bone marrow is the same result as that in hMSCs derived from adipose tissue reported by Rubio et al.[10] In addition, a decreasing cellular proliferation rate is often observed in several types of normal cells during in vitro culture. Consequently, these results suggest that hMSCs derived from bone marrow will seldom undergo spontaneous transformation during the 1–2 month period of in vitro culture necessary for use in clinical applications. But why does the proliferation of hMSCs decrease during in vitro culture? To focus on the proliferation mechanism of stem cells, we investigated whether the expressions of several genes related to cellular proliferation in hMSCs changed during in vitro culture. In the present study, we examined the expressions of TGFβs, their receptors, Smad3, c-myc, nucleostemin, and Wnt-8B. It has been proposed that the loss of TGFβRIII in renal cell carcinoma (RCC) is necessary for RCC carcinogenesis, and loss of TGFβRII leads to acquisition of the metastatic phenotype.[19] Therefore, the absence of changes in TGFβRII and TGFβRIII in hMSCs during in vitro culture might be important. The changes in mRNA expression levels during in vitro culture were different in each TGFβ isomer and receptor. TGFβ signal transduction in the cellular pathway is only possible through activation of TGFβRI. It was interesting that only TGFβRI mRNA expression increased with the length of cell culture among the three kinds of receptors (Fig. 2). The mRNA expressions of Smad3 increased (Fig. 3), but those of c-myc and nucleostemin decreased (Fig. 4) with the length of cell culture. We summarize the changes of TGFβ signaling gene expression during in vitro culture of hMSCs for 3 months in Fig. 7. TGFβ inhibits the growth of the many kinds of epithelial cells and hematopoietic, lymphoid, and endothelial cells.[20–23] In hMSCs as well as in the above-mentioned cells, hMSC growth might be controlled by TGFβ family signaling. As shown in Fig. 7, we hypothesized that the expressions of TGFβ1 and TGFβ2 in hMSCs increased during the period of in vitro culture, and then activated TGFβRI repressed the transcription of c-myc through Smad3; consequently, the cell cycle and cell growth might be arrested in hMSCs.

In addition, we compared the gene expression profiles of hMSCs with two kinds of cancer cell lines. One was HeLa S3 (a human cervical cancer cell line), which is markedly transformed, and the other was HepG2 (a human hepatoma cell line), which retains some hepatic functions. The mRNA expressions of TGFβs and their receptors in hMSCs were significantly higher than in the two types of cancer cells (HeLa S3 and HepG2) (Fig. 5). On the other hand, the mRNA expressions of c-myc and nucleostemin of the stem cells (hMSCs) were significantly lower than those of the two types of cancer cells (Fig. 6). Wnt signaling promotes self-renewal of hematopoietic, intestinal epithelial, and keratinocyte stem cells, among others;[9] however, Wnt-8B was not expressed in hMSCs derived from bone marrow (Fig. 6). These results suggest that expression of the genes that inhibit cellular proliferation and tumorigenesis were significantly higher and the genes that promote these processes were lower in hMSCs than in the cancer cells. Thus, the expression profiles of the genes that regulate cellular proliferation in hMSCs were significantly different from those of cancer cells.

## Conclusion

In the present study, we confirmed that spontaneous transformation seldom occurred in hMSCs derived from bone marrow during 1–2 months of in vitro culture for use in clinical applications. In hMSCs, as in epithelial cells, growth might be controlled by TGFβ family signaling. During the period of in vitro culture of hMSCs, the expressions of TGFβ1 and TGFβ2 increased, and then activated TGFβRI repressed the transcription of c-myc through Smad3; consequently, the cell cycle and cell growth might have been arrested in hMSCs. In addition, the expression profiles of the genes that regulate cellular proliferation in hMSCs were significantly different from those of the cancer cells.

**Acknowledgments** This work was partially supported by a grant for Research on Health Sciences Focusing on Drug Innovation from the Japan Health Sciences Foundation, and Health and Labour Sciences research grants for Research on Advanced Medical Technology from the Ministry of Health, Labour and Welfare of Japan.

## References

1. Jiang Y, Jahagirdar BN, Reinhardt RL, Schwartz RE, Keene CD, Ortiz-Gonzalez XR, Reyes M, Lenvik T, Lund T, Blackstad M, Du J, Aldrich S, Lisberg A, Low WC, Largaespada DA, Verfaillie CM. Pluripotency of mesenchymal stem cells derived from adult marrow. Nature 2002;418:41–49
2. Rosenthal N. Prometheus's vulture and the stem-cell promise. N Engl J Med 2003;349:267–274
3. Korbling M, Estrov Z. Adult stem cells for tissue repair – A new therapeutic concept? N Engl J Med 2003;349:570–582
4. Hishikawa K, Miura S, Marumo T, Yoshioka H, Mori Y, Takato T, Fujita T. Gene expression profile of human mesenchymal stem cells during osteogenesis in three-dimensional thermo-reversible gelation polymer. Biochem Biophys Res Commun 2004;317:1103–1107
5. Horwitz EM, Gordon PL, Koo WKK, Marx JC, Neel MD, McNall RY, Muul L, Hofmann T. Isolated allogenic bone marrow-derived mesenchymal cells engraft and stimulate growth in children with osteogenesis imperfecta: Implications for cell therapy of bone. Proc Natl Acad Sci USA 2002;99:8932–8937
6. Mangi AA, Noiseux N, Kong D, He H, Rezvani M, Ingwall JS, Dzau VJ. Mesenchymal stem cells modified with Akt prevent remodeling and restore performance of infarcted hearts. Nat Med 2003;9:1195–1201
7. Strauer BE, Brehm M, Zeus T, Kostering M, Hernandez A, Sorg RV, Kogler G, Wernet P. Repair of infarcted myocardium by autologous intracoronary mononuclear bone marrow cell transplantation in humans. Circulation 2002;106:1913–1918
8. Petersen BE, Bowen WC, Patrene KD, Mars WN, Sullivan AK, Murase N, Boggs SS, Greenberger JS. Bone marrow as a potential source of hepatic oval cells. Science 1999;284:1168–1170
9. Pardal R, Clarke MF, Morrison SJ. Applying the principles of stem-cell biology to cancer. Nat Rev Cancer 2003;3:895–902
10. Rubio D, Garcia-Castro J, Martin MC, Fuente R, Cigudosa JC, Lloyd AC, Bernad A. Spontaneous human adult stem cell transformation. Cancer Res 2005;65:3035–3039
11. Lopez-Casillas F, Cheifetz S, Doody J, Andres JL, Lane WS, Massague J. Structure and expression of the membrane proteoglycan betaglycan, a component of the TGF-β receptor system. Cell 1991;67:785–795
12. Esparza-Lopez J, Montiel JL, Vilchis-Landeros MM, Okadome T, Miyazono K, Lopez-Casillas F. Ligand binding and functional properties of betaglycan, a co-receptor of transforming growth factor-β superfamily. J Biol Chem 2001;276:14588–14596
13. Deng X, Bellis S, Yan Z, Friedman E. Differential responsiveness to autocrine and exogenous transforming growth factor (TGF) β1 in cells with nonfunctional TGF-β receptor type III. Cell Growth Differ 1999;10:11–18
14. Blobe GC, Schiemann WP, Pepin M-C, Beauchemin M, Moustakas A, Lodish HF, O'Connor-McCourt MD. Functional roles for the cytoplasmic domain of the type III transforming growth factor β receptor in regulating transforming growth factor β signaling. J Biol Chem 2001;276:24627–24637
15. Massague J, Wotton D. Transcriptional control by the TGF-β/Smad signaling system. EMBO J 2000;19:1745–1754
16. Moustakas A, Souchelnytskyi S, Heldin C-H. Smad regulation in TGF-β signal transduction. J Cell Sci 2001;114:4359–4369
17. Willert K, Brown JD, Danenberg E, Duncan AW, Weissman IL, Reya T, Yates JR III, Nusse R. Wnt proteins are lipid-modified and can act as stem cell growth factors. Nature 2003;423:448–452
18. Tsai RYL, McKay RDG. A nucleolar mechanism controlling cell proliferation in stem cells and cancer cells. Genes Dev 2002;16:2991–3003
19. Copland JA, Luxon BA, Ajani L, Maity T, Campagnaro E, Guo H, LeGrand SN, Tamboli P, Wood CG. Genomic profiling identifies alterations in TGFβ signaling through loss of TGFβ receptor expression in human renal cell carcinogenesis and progression. Oncogene 2003;22:8053–8062
20. Massague J, Blain SW, Lo RS. TGFβ signaling in growth control, cancer, and heritable disorders. Cell 2000;103:295–309
21. Feng XH, Lin X, Derynck R. Smad2, Smad3 and Smad4 cooperate with Sp1 to induce $p15^{Ink4B}$ transcription in response to TGF-β. EMBO J 2000;19:5178–5193
22. Yagi K, Furuhashi M, Aoki H, Goto D, Kuwano H, Sugamura K, Miyazono K, Kato M. *c-myc* is a downstream target of the Smad pathway, J Biol Chem 2002;277:854–861
23. Chen CR, Kang Y, Siegel PM, Massague J. E2F4/5 and p107 as Smad cofactors linking the TGFβ receptor to *c-myc* repression Cell 2002;110:19–32

# Effects of a biodegradable polymer synthesized with inorganic tin on the chondrogenesis of human articular chondrocytes

**Nasreen Banu, Toshie Tsuchiya, Rumi Sawada**
*Division of Medical Devices, National Institute of Health Sciences, 1–18-1 Kamiyoga, Setagaya-ku, Tokyo 158-8501, Japan*

Received 8 September 2005; accepted 14 September 2005
Published online 14 December 2005 in Wiley InterScience (www.interscience.wiley.com). DOI: 10.1002/jbm.a.30616

**Abstract:** Recent study has shown that biodegradable polymers are attractive candidates for chondrocyte fixation and further transplantation in cartilage tissue engineering. Poly (glycolic acid) (PGA), a polymer of glycolic acid, is widely used in orthopedic applications as a biodegradable polymer. Organotin, lead, antimony, and zinc are catalysts commonly used in synthesizing PGA. Here, we investigated the biocompatibility of PGA, synthesized with and without inorganic tin as a catalyst in chondrogenesis of human articular chondrocytes in a micromass culture system. Significant enhancement of chondrocyte proliferation and expression of the collagen type II protein gene were observed in cultures treated with PGA synthesized with a tin catalyst. However, aggrecan gene expression was very similar to the control culture. Amount of collagen type II protein was also increased in the same group of cultured chondrocytes. In contrast, PGA without a catalyst caused overall inhibition of chondrogenesis. Despite several positive findings, extensive investigations are essential for the feasibility of this PGA(Sn) in future clinical practice. © 2005 Wiley Periodicals, Inc. J Biomed Mater Res 77A: 84–89, 2006

**Key words:** poly (glycolic acid); inorganic tin catalyst; human articular cartilage; chondrogenesis; micromass culture

## INTRODUCTION

Different synthetic biodegradable polymers are currently gaining importance in the fields of biotechnology and tissue engineering. Recently, many studies have evaluated the potential of various natural bioabsorbable polymers such as collagen, [1,2] alginates, [3–5] fibrin, [6–8] and gelatin, [9] but synthetic biodegradable polymers in general offer advantages over natural materials. The primary advantages include the capacity to change the mechanical properties and degradation kinetics to suit various applications. Among the families of synthetic polymers, polyesters are used in a number of clinical applications.[10–12] Polyesters have also been used for development of tissue engineering applications, [13,14] particularly for bone tissue engineering.[15,12]

*Correspondence to:* T. Tsuchiya; e-mail: tsuchiya@nihs.go.jp
Contract grant sponsor: Health and Labour Sciences Research
Contract grant sponsor: Ministry of Health, Labour and Welfare (Japan)
Contract grant sponsor: Japan Health Sciences Foundation



The attraction of poly (glycolic acid) (PGA), one of the aliphatic polyesters, as a biodegradable polymer in medical applications is that its degradation product, glycolic acid, is a natural metabolite. Several studies have indicated that copolymers of glycolic acid caused promotion of nerve regeneration in a rat model, [16–18] and regeneration of an 80 mm nerve gap by an artificial nerve conduit made of PGA was also reported.[19] PGA can be synthesized using different catalysts. The common catalysts used include organotin, lead, antimony, and zinc. It was reported that inorganic and organic tin compounds present in the aqueous ecosystem have toxic effects and are capable of producing behavioral abnormalities in living organisms.[20,21] Organotin compounds are known to cause neurotoxicity, [22] cytotoxicity, [23] immunotoxicity, and genotoxicity [24] in human and other mammalian cells both *in vitro* and *in vivo*. Organotin compounds were also reported to decrease *in vitro* survival, proliferation, and differentiation of normal human B cells.[25] The dose effect of inorganic tin in rats suggests that the critical organ in inorganic tin toxicity is bone, [26] and disproportionate dwarfing syndrome, which severely affects the limbs but not the trunk, was observed in rats that had been injected with certain tin compounds.[27] As far as we know, no study yet has reported the chondrogenic

effects of PGA synthesized with and without an inorganic tin catalyst. In this study, the biocompatibility of PGA with and without a tin catalyst was investigated, using human articular chondrocytes (HAC) in a micromass culture system.

## MATERIALS AND METHODS

### Medium and polymers used for cell culture

Chondrocyte growth medium was obtained commercially from BioWhittaker (Walkersville, MD, USA). PGA synthesized with inorganic tin [PGA(Sn)] ($M_w$ = 1500) and without a catalyst (PGA) ($M_w$ = 1100) were custom-made (TAKI chemicals, Kakogawa, Japan) and dissolved in dimethyl sulphoxide (DMSO) (Sigma Chemical, St. Louis, MO, USA).

### Cells and culture methods

Human articular chondrocytes (HAC) of the knee joint was commercially obtained from BioWhittaker. High-density micromass cultures were started by spotting $4 \times 10^5$ cells in 20 μL of medium onto Costar 24-well tissue culture microplates (Costar type 3526, Corning). After a 2 h attachment period at 37°C in a $CO_2$ incubator, culture medium (1 mL/well) was added to each well. Media were supplemented with DMSO (0.8 μL/mL), PGA, and PGA(Sn) (50 μg/mL). HAC cultured with DMSO was used as the control. The cultures were continued for 4 weeks with a medium change twice a week. At least four cultures were performed for each sample.

### Cell proliferation study

Cell proliferation was quantitatively estimated by crystal violet (Wako Pure Chemical Industries, Osaka, Japan) staining, as previously described.[28] After the culture period, cells were fixed with 100% methanol at room temperature, followed by application of 0.1% crystal violet in methanol. After a proper wash, cells were again incubated in methanol; 100 μL from each well was transferred to a new 96-well plate, and the absorbance was measured at a wavelength of 590 nm, using an ELISA reader (Bio-Tek Instruments, Winooski, VT). Blank values were subtracted from experimental values to eliminate background readings.

### Differentiation assay

Cell differentiation assay was performed by alcian blue (Wako Pure Chemical Industries, Osaka, Japan) staining, as previously described.[29] Following crystal violet staining, the cells were washed with methanol and then 3% acetic acid. Cultures were then stained with 1% (v/v) alcian blue in 3% acetic acid, pH 1.0. The cartilage proteoglycans were extracted with 4*M* guanidine hydrochloride (GH), and the bound dye was measured at wavelength of 600 nm, using an ELISA reader (Bio-Tek Instruments). Fresh 4*M* GH served as the blank. Blank values were subtracted from experimental values to eliminate background readings.

### Analytical assays

Commercially available assay kits (collagen and glycosaminoglycan [GAG] assay kits, Biocolor, Newtownabbey, Northern Ireland) were used for the measurement of collagen and sulfated GAGs within the cultured cells, as previously described.[30]

Briefly, for the GAG assay, GAG was extracted from the cultured cells using a solvent system of 4*M* guanidine-HCl, 0.5*M* sodium acetate, pH 6, with 1 m*M* benzamidine-HCl, 1 m*M* phenylmethylsulfonyl fluoride (PMSF), and 10 m*M* *N*-ethylmaleimide (NEM). Incubation was carried out at 4°C on an orbital shaker for a 12- to 20-h period. After the extraction, the samples were centrifuged, and blyscan dye reagent (composed of 1,9-dimethyl methylene blue in an organic buffer) was mixed with the supernatant. The GAG–dye complex was collected by centrifugation. The dye bound to the pellet was subsequently solubilized by mixing it with a dissociation reagent. The absorbance of the samples was measured at a wavelength of 656 nm, using a UV spectrophotometer. A calibration solution containing chondroitin-4 sulfate was used to obtain the standard curve for this experiment.

The total collagen concentration (acid- and pepsin-soluble fractions) of the cultured chondrocytes was also measured. The acid-soluble collagen was removed by adding 0.5*M* acetic acid to the cultured cells, followed by centrifugation. The remaining pepsin-soluble collagen was subsequently extracted from the cultured cells. A pepsin solution (1 mg/10 mg tissue sample; Sigma) was added to the cells, and they were incubated overnight at 37°C. Both the acid- and pepsin-soluble collagen samples were further separated for assay by mixing with Sircol dye reagent for 30 min in a mechanical shaker, and the collagen–dye complex was collected by centrifugation. The dye bound to the collagen pellet was solubilized with an alkaline reagent, and the absorbance of the samples was measured at a wavelength of 540 nm, using a UV spectrophotometer. A calibration standard of acid-soluble type I collagen was used to obtain the standard curve for this experiment.

### Real-time polymerase chain reaction

To detect the presence of collagen type II and aggrecan, single-stranded cDNA was prepared from 1 μg of total RNA by reverse transcription (RT), using a commercially available First-Strand cDNA kit (Amersham Pharmacia Biotech, Uppsala, Sweden). Subsequently, real-time polymerase chain reaction (PCR) was done using a LightCycler system with LightCycler FastStart DNA Master SYBR Green I

(Roche Diagnostics, Penzberg, Germany). The LightCycler™- Primer set (Roche Diagnostics) was used for quantitative detection of the collagen type II and aggrecan genes, and also for quantitation of a housekeeping gene, Glyceraldehide-3-phosphate dehydrogenase (GAPDH), according to the manufacturer's instructions. An initial denaturation step at 95°C for 10 min was followed by amplification and extension steps for 35 cycles (95°C for 10 s, 68°C for 10 s, 72°C for 16 s) with final extension step at 58°C for 10 s. The quantification data were analyzed with the LightCycler analysis software (Roche Diagnostics).

### Statistical study

Student's $t$ tests were used to assess whether differences observed between the polymers treated and the control samples were statistically significant. For comparison of groups of means, one-way analysis of variance was carried out. When significant differences were found, Tukey's pairwise comparisons were used to investigate the nature of the difference. Statistical significance was accepted at $p < 0.05$. Values were presented as the mean ± SD (standard deviation) except in figure 3. Four samples were run for each case. All experiments were repeated at least twice, and similar results were obtained.

## RESULTS

### Cell proliferation

Chondrocyte proliferation was quantified by crystal violet staining and expressed as a percentage of the average control value (Fig. 1). Cell proliferation was increased 1.8-fold ($p < 0.05$) in PGA(Sn)-treated cultures compared with that of the control culture, whereas cell proliferation in PGA-treated cultures was almost identical to the DMSO-treated control culture.

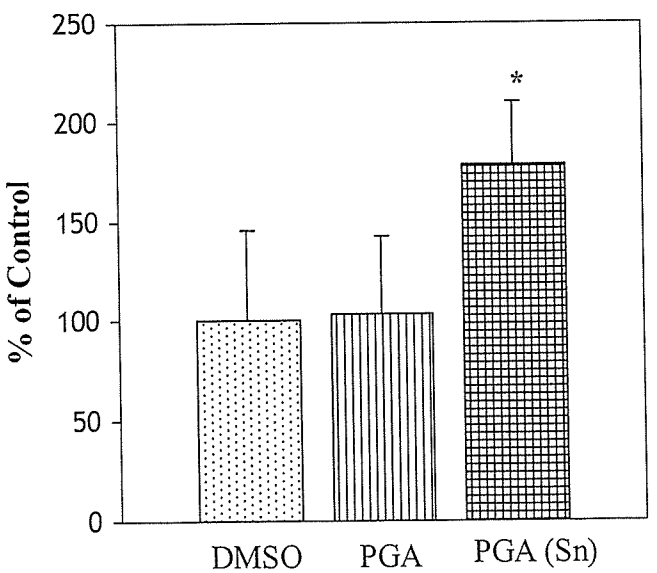


**Figure 1.** Proliferation of HAC estimated by crystal violet staining. Cell proliferation was significantly increased in PGA(Sn)-cultured chondrocytes compared with that of the control. *$p < 0.05$. All experiments were run in quadruplicate for two separate times.

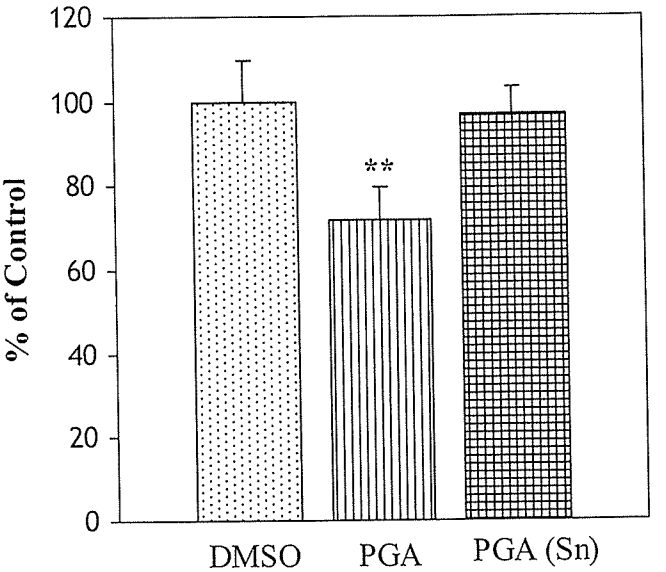


**Figure 2.** Differentiation of HAC estimated by alcian blue method. Cell differentiation was significantly inhibited in PGA-cultured chondrocytes compared with that of the control. **$p < 0.01$. All experiments were run in quadruplicate for two separate times.

### Cell differentiation

Chondrocyte differentiation was estimated by alcian blue staining and the amounts were expressed as a percentage of the average control value, which was calculated as 100%. Chondrocytes treated with PGA revealed a 0.71-fold ($p < 0.01$) decrease in cell differentiation compared with that of the control culture. At the same time, cultures treated with PGA(Sn) showed a slight, but nonsignificant, decrease in cell differentiation (Fig. 2).

### Extracellular matrix gene expression

Extracellular matrix gene expression was quantitatively measured by real-time PCR. Here, compared with that of the control culture, the collagen type II gene was more strongly expressed ($p < 0.01$) in PGA(Sn) than in PGA-treated cultured chondrocytes [Fig. 3(A)]. Aggrecan gene expression was inhibited in the latter, but no difference was observed between the former and the control culture [Fig. 3(B)].

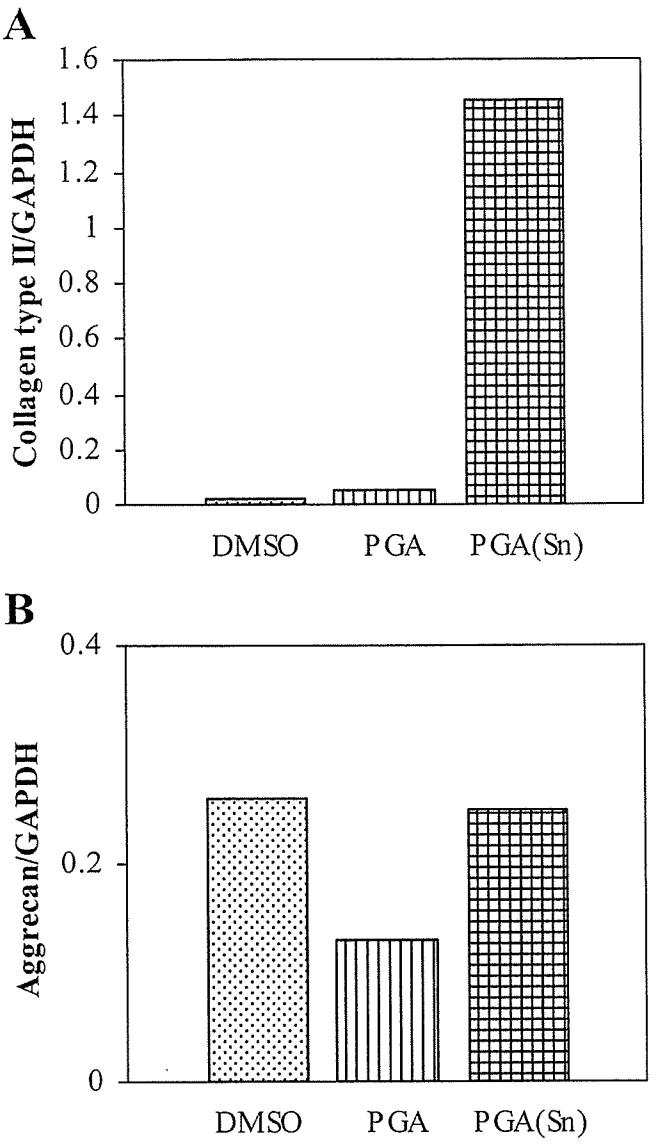


**Figure 3.** Extracellular matrix gene expression of HAC by real-time PCR. (A) Collagen type II gene was more strongly expressed in PGA(Sn)- than PGA-cultured chondrocytes compared with that of the control culture. (B) Aggrecan gene expression was inhibited in PGA, but no difference was observed between the PGA(Sn) and the control. All experiments were run in quadruplicate for two separate times.

### Measurement of collagen type II protein

The amount of pepsin-soluble and cartilage-specific collagen type II protein was increased in both PGA and PGA(Sn) treated chondrocytes on comparing with that of the control culture(Fig. 4). However, this increase was more in the latter than in the former case.

### Measurement of total collagen

Quantitative estimations of both acid- and pepsin-soluble total collagen revealed a decrease in PGA(Sn)-treated cultures compared with that of the control

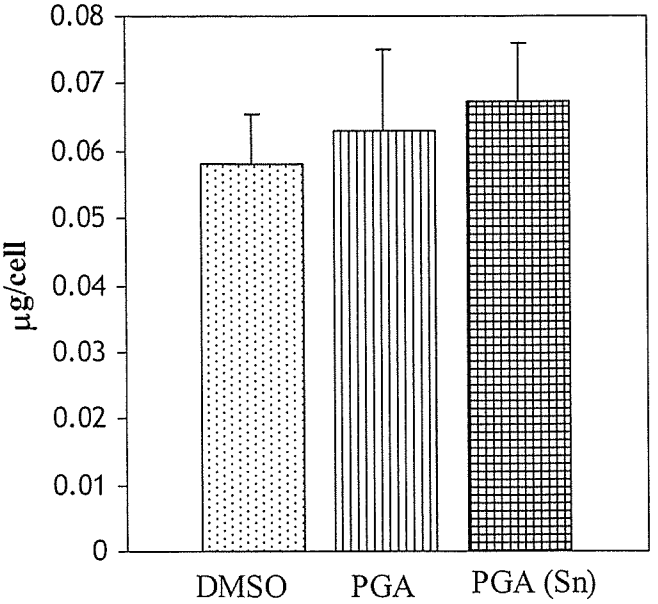


**Figure 4.** Measurement of collagen type II protein. The amount of collagen type II was increased in PGA(Sn)-treated chondrocytes compared with that of control. All experiments were run in quadruplicate for two separate times.

(Fig. 5). Simultaneously, there was a slight increase in the amount of total collagen in PGA-treated cultures compared with that of the control sample.

### Estimation of sulfated glycosaminoglycan concentration

Evaluation of the amount of sulfated GAG showed a decrease in PGA(Sn)-treated cultured cells com-

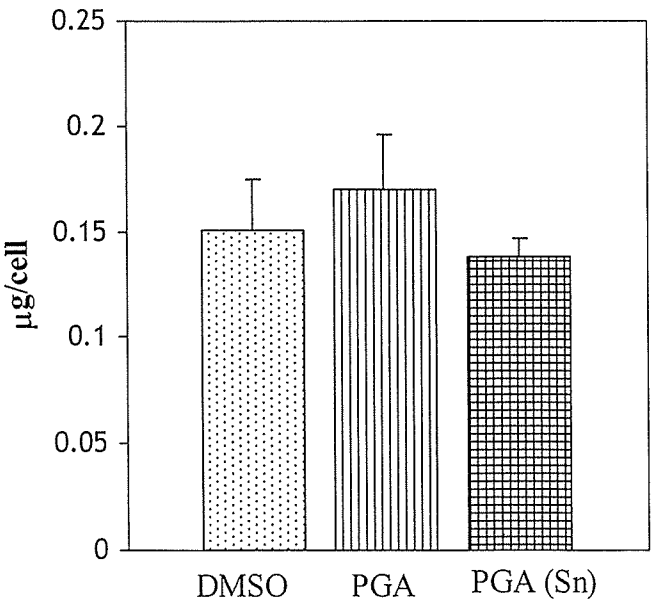


**Figure 5.** Quantitative estimation of total collagen protein. The amount of total collagen was decreased in PGA(Sn)-treated cultures compared with that of the control. All experiments were run in quadruplicate for two separate times.

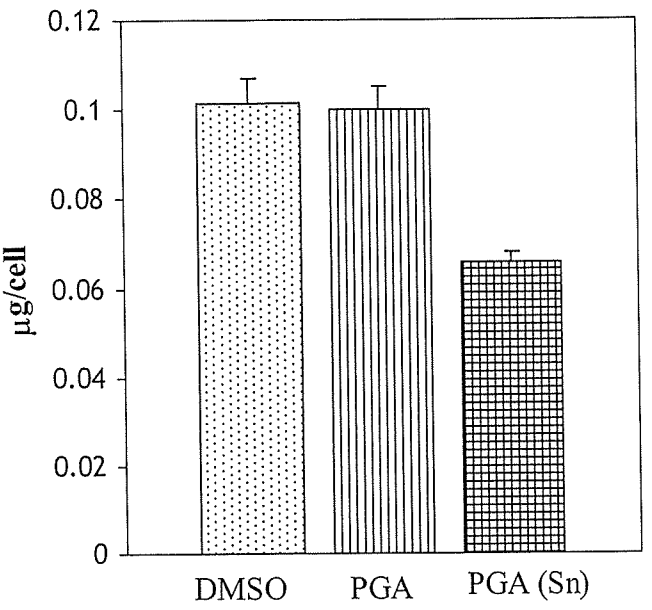


**Figure 6.** Evaluation of sulfated GAG. There was decrease in the amount of sulfated GAG in PGA(Sn)-treated cultured cells compared with that of the control. All experiments were run in quadruplicate for two separate times.

pared with that of the control (Fig. 6). However, in the same experiment, almost no difference in this amount was observed between the PGA-treated culture and the control.

## DISCUSSION

Attempts to identify a perfectly biocompatible and biodegradable polymer have been ongoing over the past decade. An ideal biomaterial should fulfill its purpose satisfactorily and then biodegrade to obviate any risk of foreign body reaction.[31] Synthetic biodegradable polymers, especially those belonging to the polyester family, have played an important role in a number of tissue engineering efforts. PGA, an aliphatic polyester, can be degraded in two ways: by hydrolysis and by nonspecific esterases and carboxypeptidases, followed by either excretion in the urine or entrance into the tricarboxylic acid cycle.[32]

Several different catalysts, namely organotin, antimony, zinc, and lead, are used in the polymerization process to synthesize high molecular weight PGA. Different tin compounds were observed to produce general cytotoxic effects in rabbit articular cartilage in monolayer culture, [33] and bone is suggested to be the critical organ in inorganic tin toxicity in rats.[26] Therefore, in this study, we aspired to evaluate the chondrogenic effects of HAC with PGA synthesized with and without an inorganic tin catalyst, with the aim of clarifying the biocompatibility of inorganic tin as a catalyst for future clinical use.

It was reported that oral administration of certain tin compounds at specific concentrations exerted stimulatory effects on chondrocyte proliferation in the rat.[33] Consistent with this, the proliferation assay performed in our study also showed that HAC with PGA(Sn) had stimulatory effects on chondrocyte proliferation in micromass culture (Fig. 1). On the other hand, PGA neither stimulated nor inhibited the chondrocyte proliferation, and thus, inorganic tin as catalyst seemed to play a stimulatory role in HAC proliferation. In our experiment, PGA with inorganic tin as the catalyst caused almost no change in cell differentiation, but PGA-treated cultures did show a significant decrease when compared with that of the control (Fig. 2). Furthermore, quantitative estimation of extracellular matrix gene expression by real-time PCR confirmed that the cartilage-specific protein, collagen type II, was more strongly expressed in PGA(Sn)- than in PGA-treated cultured chondrocytes [Fig. 3(A)]. However, the expression of the aggrecan gene was inhibited in the PGA culture, but no difference was observed between the PGA(Sn) and the control cultures [Fig. 3(B)].

It was reported that oral administration of inorganic tin caused a decrease in the proliferation of chondrocytes, accompanied by suppression of DNA synthesis with subsequent inhibition in collagen synthesis in rat.[34] On the contrary, our results showed enhancement of proliferation, expression of the collagen type II gene, and amount of collagen type II protein by *in vitro* culture of HAC with PGA(Sn). We speculated that difference in the route of administration might be the cause of these diverse effects of inorganic tin compound. As mentioned earlier, monolayer culture of rabbit articular cartilage with tin compounds caused inhibition in the synthesis of core proteins, followed by a decrease in the synthesis of sulfated GAG.[33] In agreement with this result, our report also showed a decrease in the amount of sulfated GAG by culture of HAC with PGA(Sn). A study performed in our laboratory using HAC in a micromass culture system has already shown that PGA synthesized with organic tin catalyst caused a decrease in cell proliferation, but a significant increase in cell differentiation [29] and was completely contradictory to our present results. The molecular weight of PGA(Sn), and the type of tin product such as $SnCl_2$ and dibutyl tin were thought to be the key factor of different effects of chondrogenesis on HAC.

To the best of our knowledge, no other study has yet investigated the chondrogenic effects of PGA with inorganic tin as a catalyst, using HAC in a micromass culture system. This study is the first to show the biological action of inorganic tin as catalyst in PGA on human articular chondrogenesis in a micromass culture system. Our observation revealed that low concentration of inorganic tin when used in the polymer

of PGA showed enhancing effects of tin compounds on chondrocytes in comparison to without tin polymer because of increase in the permeability of inorganic tin under the presence of PGA. However, further study is required for the application of this PGA(Sn) in clinical practice.

## References


1. Yasui N, Osawa S, Ochi T, Nakashima H, Ono K. Primary culture of chondrocytes embedded in collagen gels. Exp Cell Biol 1982;50:92–100.
2. Kimura T, Yasui N, Ohsawa S, Ono K. Chondrocytes embedded in collagen gels maintain cartilage phenotype during long-term cultures. Clin Orthop 1984;186:231–239.
3. Grandolfo M, D'Andrea P, Paoletti S, Martina M, Silvestrini G, Bonucci E, Vittur F. Culture and differentiation of chondrocytes entrapped in alginate gels. Calcif Tissue Int 1993;52:42–48.
4. Loty S, Sautier JM, Loty C, Boulekbache H, Kokubo T, Forest N. Cartilage formation by fetal rat chondrocytes cultured in alginate beads: a proposed model for investigating tissue-biomaterial interactions. J Biomed Mater Res 1998;42:213–222.
5. Perka C, Spitzer RS, Lindenhayn K, Sittinger M, Schultz O. Matrix-mixed culture: new methodology for chondrocyte culture and preparation of cartilage transplants. J Biomed Mater Res 2000;49:305–311.
6. Meinhart J, Fussenegger M, Hobling W. Stabilization of fibrin-chondrocyte constructs for cartilage reconstruction. Ann Plast Surg 1999;42:673–678.
7. Perka C, Schultz O, Lindenhayn K, Spitzer RS, Muschik M, Sittinger M, Burmester GR. Joint cartilage repair with transplantation of embryonic chondrocytes embedded in collagen-fibrin matrices. Clin Exp Rheumatol 2000;18:13–18.
8. Perka C, Schultz O, Spitzer RS, Lindenhayn K, Burmester GR, Sittinger M. Segmental bone repair by tissue-engineered periosteal cell transplants with bioresorbable fleece and fibrin scaffolds in rabbits. Biomaterials 2000;21:1145–1153.
9. George-Weinstein M, Gerhart JV, Foti GJ, Lash JW. Maturation of myogenic and chondrogenic cells in the preosmitic mesoderm of the chick embryo. Exp Cell Res 1994;211:263–274.
10. Ashammakhi N, Rokkanen P. Absorbable polyglycolide devices in trauma and bone surgery. Biomaterials 1997;18:3–9.
11. Middleton JC, Tipton JA. Synthetic biodegradable polymers as orthopedic devices. Biomaterials 2000;21:2335–2346.
12. Kohn J, Langer R. Bioresorbable and bioerodible materials. In: Ratner BD, Hoffman AS, Schoen FJ, Lemon JE, editors. An Introduction to Materials in Medicine. San Diego: Academic Press; 1997. p 65–73.
13. Wong WH, Mooney DJ. Synthesis and properties of biodegradable polymers used as synthetic matrices for tissue engineering. In: Atala A, Mooney D, editors. Synthetic Biodegradable Polymer Scaffolds. Boston: Burkhauser; 1997. p 51–84.
14. Yaszemsky MJ, Payne RG, Hayes WC, Langer R, Mikos AG. Evolution of bone transplantation: Molecular, cellular and tissue strategies to engineer human bone. Biomaterials 1996;17:175–185.
15. Burg KJL, Porter S, Kellam JF. Biomaterials development for bone tissue engineering. Biomaterials 2000;21:2347–2359.
16. Tessa H, Sundback C, Hunter D, Cheney M, Vacanti JP. A polymer foam conduit seeded with Schwann cells promoted guided peripheral nerve regeneration. Tissue Eng 2000;6:119–127.
17. Bryan DJ, Holway AH, Wang KK, Silva AE, Trantolo DJ, Wise D, Summerhayes IC. Influence of glial growth factor and Schwann cells in a bioresorbable guidance channel on peripheral nerve regeneration. Tissue Eng 2000;6:129–138.
18. Evans GRD, Brandt K, Widmer MS, Lu L, Meszlenyi RK, Gupta PK, Mikos AG, Hodges J, Williams J, Gurlek A, Nabawi A, Lohman R, Patrick JCR. In vivo evaluation of poly(L-lactic acid) porous conduits for peripheral nerve regeneration. Biomaterials 1999;20:1109–1115.
19. Matsumoto K, Ohnishi K, Sekine T, Ueda H, Yamamoto Y, Kiyotani T, Nakamura T, Endo K, Shimizu Y. Use of a newly developed artificial nerve conduit to assist peripheral nerve regeneration across a long gap in dogs. ASAIO J 2000;46:415–420.
20. Salanki Y, D'eri Y, Platokhin A, Sh-Rozsa K. The neurotoxicity of environmental pollutants: the effect of tin (Sn2+) on acetylcholine-induced currents in growing pond snail neurons. Neurosci Behav Physiol 2000;30:63–73.
21. Gyori J, Platoshyn O, Carpenter DO, Salanki J. Effect of inorganic and organic tin compounds on Ach- and voltage-activated Na currents. Cell Mol Neurobiol 2000;20:591–604.
22. Chang LW. The neurotoxicology and pathology of organomercury, organolead, and organotin. J Toxicol Sci 1990;15:125–151.
23. de Mattos JC, Dantas FJS, Bezerra RJAC, Bernardo-Filho M, Cabral-Neto JB, Lage C, Leitao AC, Caldeira-de-Araujo A. Damage induced by stannous chloride in plasmid DNA. Toxicol Lett 2000;116:159–163.
24. Chao JS, Wei LY, Huang MC, Liang SC, Chen HH. Genotoxic effects of triphenyltin acetate and triphenyltin hydroxide on mammalian cells in vitro and in vivo. Mutat Res 1999;21:167–174.
25. De Santiago A, Aguilar-Santelises M. Ogranotin compounds decrease in vitro survival, proliferation and differentiation of normal human B lymphocytes. Hum Exp Toxicol 1999;18:619–624.
26. Yamaguchi M, Kitade M, Okada S. The oral administration of stannous chloride to rats. Toxicol Lett 1980;5:275–278.
27. Chang LW. Hippocampal lesions induced by trimethyltin in neonatal rat brain. Neurotoxicology 1984;5:205–215.
28. Tsuchiya T, Ikarashi Y, Arai T, Ohhashi J, Nakamura A. Improved sensitivity and decreased sample size in a cytotoxicity test for biomaterials: a modified colony microassay using a microplate and crystal violet staining. J Appl Biomater 1994;5:361–367.
29. Rahman MS, Tsuchiya T. Enhancement of chondrogenic differentiation of human articular chondrocytes by biodegradable polymers. Tissue Eng 2001;7:781–790.
30. Brown AN, Kim BS, Alsberg E, Mooney DJ. Combining chondrocytes and smooth muscle cells to engineer hybrid soft tissue constructs. Tissue Eng 2000;6:297–305.
31. Gristina AG. Biomaterial-centered infection: microbial adhesion versus tissue integration. Science 1987;237:1588–1595.
32. William SDF. Some observations on the role of cellular enzymes in the *in vivo* degradation of polymers. In: Syrett BC, Acharya A, editors. Corrosion and degradation of implant materials 1979. p 61–75.
33. Webber RJ, Dollins SC, Harris M, Hough AJ Jr. Effect of alkyltins on rabbit articular and growth-plate chondrocytes in monolayer culture. J Toxicol Environ Health 1985;16:229–242.
34. Yamaguchi M, Sugii K, Okada S. Inhibition of collagen synthesis in the femur of rats orally administered stannous chloride. J Pharm Dyn 1982;5:388–393.

Available online at www.sciencedirect.com
SCIENCE DIRECT
Journal of Clinical Neuroscience 13 (2006) 250–256
Journal of Clinical Neuroscience
www.elsevier.com/locate/jocn

Laboratory study

# Coordinate expression of BMP-2, BMP receptors and Noggin in normal mouse spine

Yukio Nakamura, Hiroyuki Nakaya, Naoto Saito, Shigeyuki Wakitani *

*Department of Orthopaedic Surgery, Shinshu University School of Medicine, Asahi 3-1-1, Matsumoto, 390-8621, Japan*

Received 25 August 2004; accepted 31 May 2005

**Abstract**

The purpose of this study was to determine the localization of bone morphogenetic protein-2 (BMP-2), BMP receptors (BMPRs) and Noggin in mouse spinal tissues. The coordinate expression of these positive and negative regulators of BMP signaling may elucidate regulatory mechanisms for bone induction in the spine. Whole spines from 3-week-old mice were used and the spatial expression profiles of BMP-2, BMPR-1a, -1b, -2 and Noggin were examined using in situ hybridization. BMP-2, BMPR-1b and -2 were observed in bone marrow cells in the vertebrae, chondrocytes, hyaline cartilage cells and fibrous cells in the intervertebral discs and neurons of the spinal cord in the entire spine. BMPR-1a was also observed in these cells, but only in the cervical spine. Noggin was expressed in bone marrow cells in the vertebrae, chondrocytes and hyaline cartilage cells and fibrous cells in the intervertebral discs in the entire spine and in neurons in the spinal cord in the cervical and thoracic regions. Noggin was also expressed in the anterior longitudinal, posterior longitudinal and yellow ligaments in the cervical spine, and in the fibrous cells in the anterior longitudinal and yellow ligaments of the lumbar spine.


*Keywords:* BMP-related molecules; In situ hybridization; Localization; Spine

## 1. Introduction

Signaling by BMPs requires binding of the BMP molecules (BMP-2, -4 and -7) to one of two types of serine-threonine BMP receptors (BMPRs), known as type 1 (1a and 1b) and type 2 BMPR.[1] These receptors then phosphorylate intra-cellular proteins, including the Smads (Smad 1–5) to effect intracellular signaling and physiological responses.[2–5] Therefore, BMPR expression is a prerequisite for biological action of BMP. An important growth factor related to BMP and BMPR is Noggin, a molecule that has been shown to antagonize the action of the BMPs.[6–9] The coordinate expression of these positive and negative regulators of BMP signaling points to a potential regulatory mechanism for bone induction.

BMPs are involved in the morphogenesis and development of many organ systems. The expression of BMPR-1a or -1b has been reported during bone formation in fracture repair and pathological ectopic bone formation in spinal ligaments.[3,5,10] BMPs also play a key role in the development and growth of neurons, bone and cartilage, therefore, they may be important in the morphogenesis of spinal systems. There is also evidence from animal models that BMPs play a role in diseases characterised by mineralization of ligaments, including ossification of the anterior or posterior longitudinal ligament, ankylosing spondylitis, ossification of the ligamentum flavum and spinal spondylosis. However, there have been no reports published to date that show the distribution of BMP-2, BMPR or Noggin in normal animal models using whole spinal tissue.[11–13] Although previous reports have described aspects of spinal ossification, little is known about the molecular mechanisms that drive this event in spinal tissue.

Therefore, we used in situ hybridization to define the spatial expression profiles and localization of BMP-2, BMPRs, and Noggin in the whole spine of normal mice.

* Corresponding author. Tel.: +81 263 37 2659; fax: +81 263 35 8844.
*E-mail address:* wakitani@hsp.md.shinshu-u.ac.jp (S. Wakitani).

0967-5868/$ - see front matter © 2006 Elsevier Ltd. All rights reserved.
doi:10.1016/j.jocn.2005.05.011

## 2. Materials and methods

### 2.1. Histological preparation

Three-week-old male ddY mice were used, purchased from Nippon SLC Co. (Shizuoka, Japan) and housed in cages with free access to food and water for 1 week prior to sacrifice. Mice were sacrificed with diethyl ether.

Specimens were removed en bloc and fixed in 10% neutral buffered formalin. They were decalcified with 20% EDTA after washing with 0.1 mol/L phosphate-buffered saline (PBS). They were then dehydrated through graded ethanol, and embedded in paraffin. Sections of 4-μm thickness were prepared using a microtome, and processed for hematoxylin and eosin (*H/E*) staining.

### 2.2. RNA probes for in situ hybridization

A 0.50-kilobase (kb) fragment of mouse BMPR-1a cDNA, a 0.47-kb fragment of mouse BMPR-1b cDNA, a 0.55-kb fragment of mouse BMPR-2 cDNA, and a 0.32-kb fragment of mouse Noggin cDNA were used as templates to synthesize RNA probes. They were subcloned into pBluescript SK (+) plasmid (Stratagene, La Jolla, CA). The BMP-2 and Noggin cDNAs were obtained by reverse transcription polymerase chain reaction (RT-PCR), and the Noggin primers for PCR were as described previously.[14] The BMPR primers for PCR were as follows: BMPR-1a: 5′-CTCATGTTCAAGGGCAG-3′ (5′ sense) and 5′-CCCCTGCTTGAGATACTC-3′ (3′ antisense; 346–362 and 850-833, respectively). BMPR-1b: 5′-ATGTGGGCACCAAGAAG-3′ and 5′-CTGCTCC-AGCCCAATGCT-3′ (215-231 and 681-664, respectively). BMPR-2: 5′- GTGCCCTGGCTGCTATGG-3′ and 5′-TGCCGCCTCCATCATGTT-3′ (47-64 and 592-575, respectively). Nucleotide sequences of the cDNA fragments were checked and found to be identical to mouse BMPRs (BMPR-1a: NM009758, BMPR-1b: NM007560, BMPR-2: NM007561).

For in situ hybridization, each plasmid containing a BMP-2 or Noggin cDNA fragment was linearized as described previously.[14] Plasmids with BMPR cDNA fragments were either linearised with *Xba I* and transcribed with T3 RNA polymerase to generate long antisense RNA probes or linearised with *Xho I*, and transcribed with T7 RNA polymerase to generate sense RNA probes.

### 2.3. In situ hybridization

In situ hybridization was carried out as described previously.[14,15] Mice were sacrificed and fixed by vascular perfusion with 4% paraformaldehyde (PFA). Tissue specimens were then removed, and fixed in fresh PFA solution for 24 hours. After fixation, the tissues were embedded in paraffin, and 7-μm sections were cut and then mounted on sialinized, APS-coated slides. They were stored at 4 °C until use. Sections were blow-dried, deparaffinized, rehydrated, and fixed with 4% PFA for 10 min at room temperature. They were then treated with PBS for 5 min, Proteinase K (15 μg/mL) in PBS for 10 min at 37 °C, 4% PFA for 10 min, 0.2N HCl for 10 min, 0.1 mol triethanolamine for 5 min and 1% acetic acid 0.1 mol triethanolamine for 10 min at room temperature. The hybridization solution contained 50% deionized formamide, 5x SSC, 1% SDS, 50 μ/mL heparin and approximately 75 ng/slide of RNA probe. Digoxigenin (DIG)-labeled single-strand antisense RNA probes for BMP-2, BMPR-1a, -1b, -2 and Noggin prepared with a DIG-labeling Mix (x10 concentration) were hybridized with the histological sections, covered with siliconized coverglasses, and incubated at 60 °C for 16 hours in a humid chamber. After hybridization, the slides were washed for 10 min twice with 2x SSC at 50 °C, and 0.2x SSC at 50 °C. Hybridised DIG-labelled probes were detected using Tris buffered saline (TBS) (0.3% Tween 20), blocking solution, anti DIG-alkaline phosphatase-labelled antibody (1:2000), TBS (0.3% Tween 20) twice, APB buffer (0.1 M Tris-HCl (Ph 9.5), 0.1 M NaCl, 50 mM $MgCl_2$), and then developed with NBT/BCIP substrate. Thereafter, the slides were mounted with Kernechtrot stain solution (Muto Chemical Co., Tokyo, Japan).

The controls consisted of hybridization with the sense probes and omission of either the antisense RNA probe or the anti-DIG antibody.

This study was carried out in accordance with the World Medical Association Declaration of Helsinki.

## 3. Results

### 3.1. Expression of BMP-2

BMP-2 was moderately and broadly detected in bone marrow cells in vertebral bone in the cervical, thoracic and lumbar spine. It was weakly detected in chondrocytes, hyaline cartilage cells and fibrous cells in the intervertebral discs in the cervical, thoracic, and lumbar spine. This pattern of moderate staining was repeated in the neurons of the spinal cord and it was also weakly detected in fibrous cells in parts of the yellow ligament in the cervical, thoracic and lumbar spine (Fig. 1A, B).

### 3.2. Expression of BMPR-1a

In the cervical spine, BMPR-1a was stained lightly and diffusely in bone marrow cells in vertebral bone, but not in the intervertebral discs. A moderate and more focused pattern of staining was observed in the neurons in the spinal cord. BMPR-1a was stained in the fibrous cells in the yellow ligament, but not in the anterior or posterior longitudinal ligaments. No staining for BMPR-1a was observed in any part of the thoracic or lumbar spine or the surrounding tissues (data not shown).

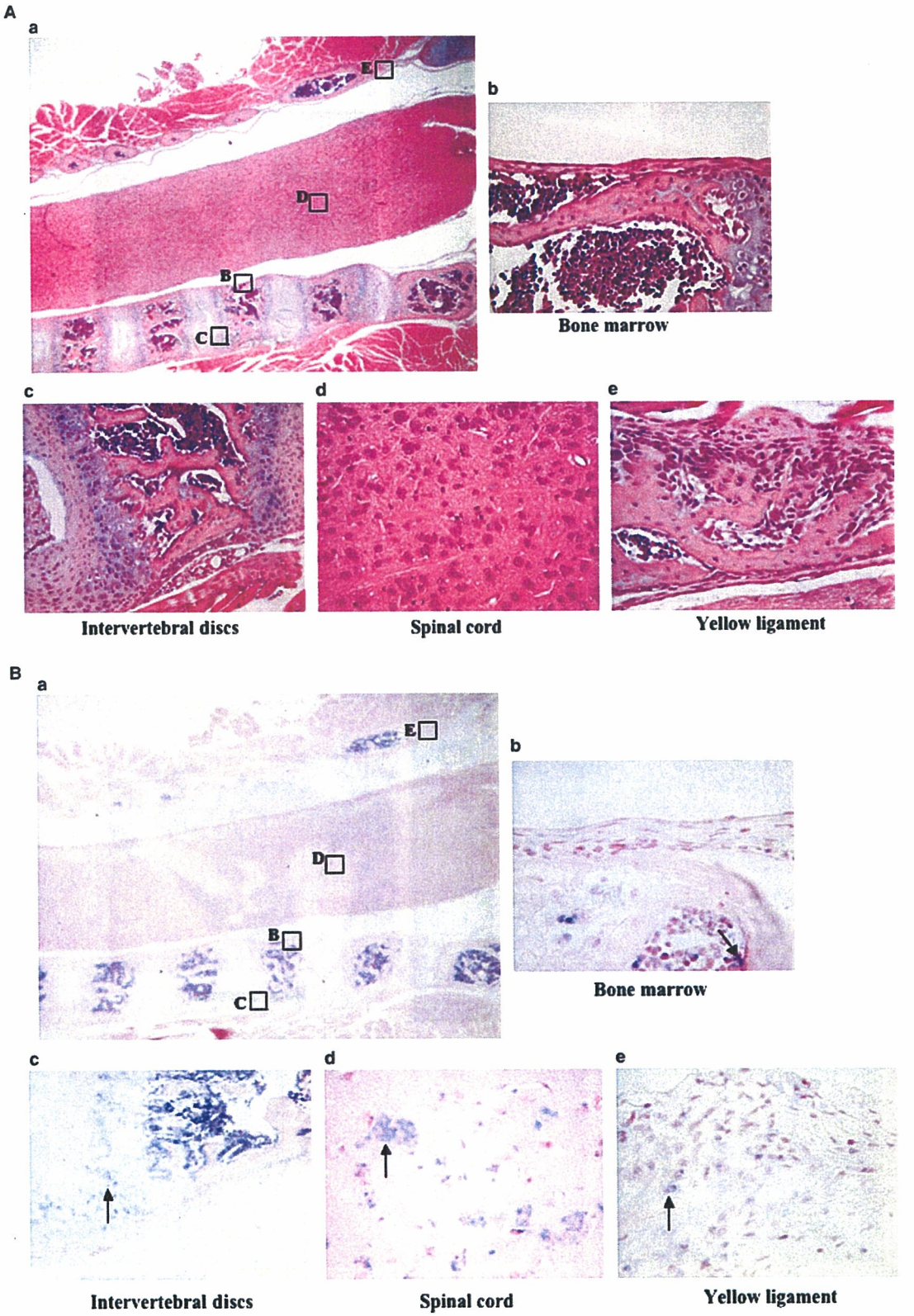


Fig. 1A. (a) Hematoxylin and eosin histochemistry of the cervical spine of the 3-week-old mouse corresponding to in situ hybridization of BMP-2 in Fig. 1B. (b) In situ hybridization of BMP-2 in the cervical spine of the 3-week-old mouse. In the whole cervical spine (a: original magnification: ×16), vertebral bone (b: original magnification: ×400), intervertebral discs (c: original magnification: ×400), spinal cord (d: original magnification: ×400) and yellow ligament (e: original magnification: ×400). Arrow in (b) indicates moderate expression in bone marrow cells and arrows in (c) indicate weak expression in hyaline cartilage cells. Arrow in (d) indicates moderate expression in neurons and arrows in (e) indicate weak staining of fibrous cells.

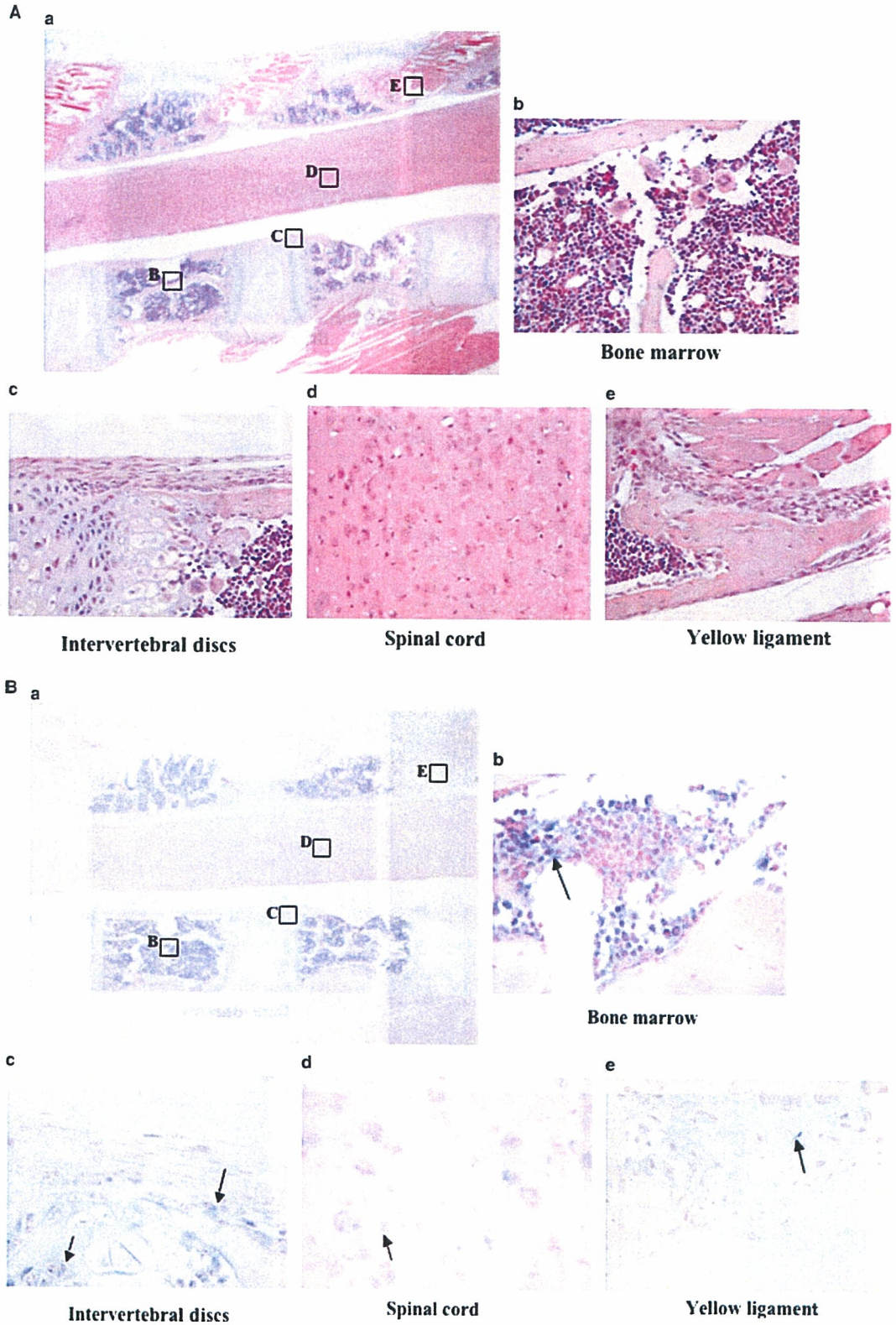


Fig. 2A. (a) Hematoxylin and eosin histochemistry of the lumbar spine of the 3-week-old mouse corresponding to in situ hybridization of BMPR-1b in Fig. 2B. (b) In situ hybridization of BMPR-1b in the lumbar spine of the 3-week-old mouse. In the whole lumbar spine (a: original magnification: ×16), vertebral bone (b: original magnification: ×400), intervertebral discs (c: original magnification: ×400), spinal cord (d: original magnification: ×400) and yellow ligament (e: original magnification: ×400). Arrow in (b) indicates strong expression in bone marrow cells and arrows in (c) indicate moderate expression in osteoblastic cells, multinuclear chondrocytes and hyaline cartilage cells. Arrow in (d) indicates moderate expression in neurons and arrows in (e) indicate weak staining of fibrous cells.

### 3.3. Expression of BMPR-1b

BMPR-1b was strongly and broadly detected in bone marrow cells, diffusely in osteoblastic cells and multinuclear cells in the vertebral bone of the cervical, thoracic and lumbar spine. It was also moderately stained in chondrocytes, hyaline cartilage cells, and fibrous cells in the intervertebral discs in the cervical, thoracic and lumbar spine. This pattern of staining was repeated in the neurons of the spinal cord in the cervical, thoracic and lumbar spine. It was also stained in fibrous cells in parts of the yellow ligament, but only in the lumbar spine (Fig. 2A, B).

### 3.4. Expression of BMPR-2

In the whole spine, BMPR-2 was stained lightly and diffusely in bone marrow cells in vertebral bone and in chondrocytes, hyaline cartilage cells and fibrous cells in the intervertebral discs. Moderate staining was observed in neurons in the spinal cord, however BMPR-2 was not observed in the ligaments (data not shown).

### 3.5. Expression of Noggin

Noggin was strongly and broadly detected in bone marrow cells in vertebral bone, moderately in chondrocytes, hyaline cartilage cells and fibrous cells in intervertebral discs, the neurons in the spinal cord in cervical spine and only weakly in parts of the anterior longitudinal, posterior longitudinal and yellow ligaments. It was also stained weakly in bone marrow cells in vertebral bone, chondrocytes, hyaline cartilage cells and fibrous cells in the intervertebral discs and moderately in neurons of the spinal cord in the thoracic spine. It was stained in bone marrow cells in vertebral bone, chondrocytes, hyaline cartilage cells and fibrous cells in intervertebral discs, and in the fibrous cells in parts of the anterior longitudinal and yellow ligaments in the lumbar spine (Fig. 3A, B).

## 4. Discussion

The expression and distribution of BMP-2, BMPR-1b and -2 was confined to bone marrow cells in vertebral bone, chondrocytes, hyaline cartilage cells and fibrous cells in the intervertebral discs and neurons of the spinal cord in the entire spine. BMPR-1a was expressed similarly in those cells, but only very weakly in the cervical spine. These results suggest the coordinate expression of BMP-2, BMPR-1b and -2 might be associated with the development of the spine. BMPR-1a and -1b share approximately 85% amino acid sequence identity,[2] but each receptor has a different function. BMPR-1a and -2 are expressed ubiquitously in various tissues, and are essential for proper regulation of the later stage of chondrocyte differentiation. BMPR-1b is observed mainly in the brain in animal models, and is necessary for the early stages of mesenchymal condensation and cartilage formation. This receptor is also involved in BMP-mediated programmed cell death.[1,2] In addition, co-expression of BMPR-2 with BMPR-1a or -1b increases binding affinity, and dramatically enhances biological activity.[3]

Noggin is a specific antagonist of BMPs, and blocks the binding of BMP to the BMPRs and thus, the subsequent actions of this protein.[14] In our study, Noggin was strongly expressed in bone marrow cells in vertebral bone, with a more moderate level in chondrocytes, hyaline cartilage cells and fibrous cells in intervertebral discs and in the neurons in the spinal cord of the cervical spine. In the thoracic spine, Noggin was also observed weakly in bone marrow cells in vertebral bone and chondrocytes, hyaline cartilage cells and fibrous cells in the intervertebral discs. A similar pattern of staining was also noted in the lumbar spine. There have been no published reports regarding the localization of Noggin in mice spinal tissues to date. The expression of Noggin in normal spinal tissues documented in this study points to the possibility of a negative feedback mechanism for BMP stimulation.

In ligaments, BMPR-1a was stained in the fibrous cells in the yellow ligament of the cervical spine, BMP-2 in the fibrous cells in the yellow ligament of the entire spine, BMPR-1b in the fibrous cells in the yellow ligament of the lumbar spine and BMPR-2 expression was not observed. Noggin was expressed weakly in parts of the anterior longitudinal, posterior longitudinal and yellow ligaments in the cervical spine and also in the fibrous cells in parts of the anterior longitudinal and yellow ligaments in the lumbar spine. In summary, these results indicate that the expression of BMP-2 in the whole spine, BMPR-1a and Noggin in the cervical spine, BMPR-1b and Noggin in lumbar spine might have a relationship with the ossification of ligaments.

The central nervous system is organized mainly by neurons, astrocytes and oligodendrocytes. Neurons form a large network with axons, astrocytes and oligodendrocytes. Astrocyte differentiation is induced synergistically by BMP-2 and leukemia inhibitory factor in the developing brain. Fetal mouse brain cells can be changed from neuroepithelial cells to astrocytes in their developmental pathway by the exposure to BMP-2 as described previously.[16] It has been reported that Noggin is necessary to create neurons from neuroepithelial cells.[17] After spinal injury, neural stem cells differentiate into astrocytes, not into neurons. The up-regulation of BMP-2 or -7 after spinal injury may inhibit differentiation into neurons and promote that of astrocytes. In addition, stimulation by Noggin is thought to accelerate degeneration of neurons in spinal tissue after spinal injury.[18,19] However, the relationship between neurons and BMP-related molecules has not yet been fully established, particularly in the spinal cord. In the present study, BMP-2, BMPRs and Noggin were moderately stained in neurons in the spinal cord, indicating that BMP signaling might be related to spinal cord development.

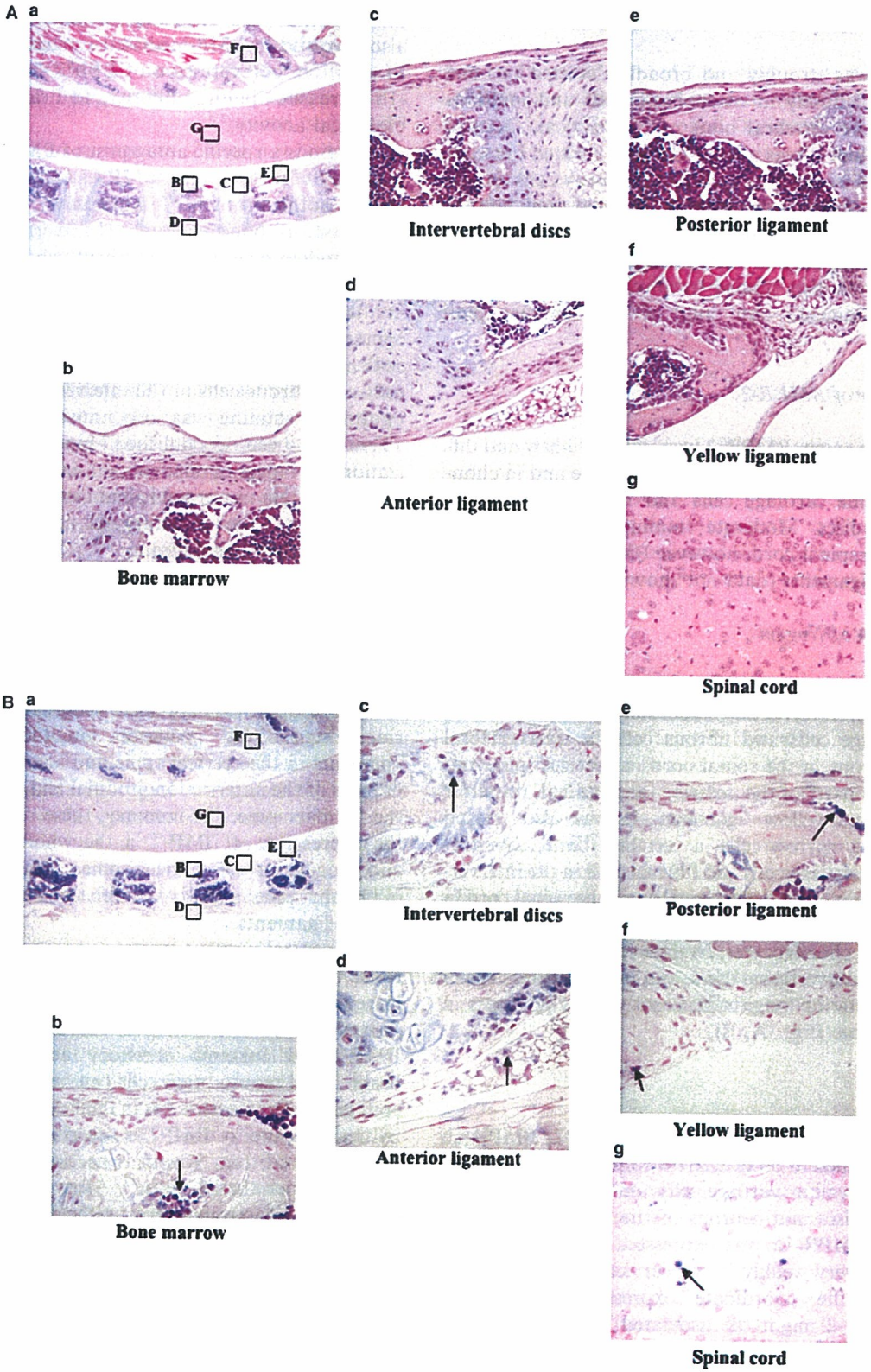


Fig. 3A. (a) Hematoxylin and eosin histochemistry of the cervical spine of the 3-week-old mouse corresponding to in situ hybridization of Noggin in Fig. 3B. (b) In situ hybridization of Noggin in the cervical spine of the 3-week-old mouse. In the whole cervical spine (a: original magnification: ×16), vertebral bone (b: original magnification: ×400), intervertebral discs (c: original magnification: ×400), anterior longitudinal ligament (d: original magnification: ×400), posterior longitudinal ligament (e: original magnification: ×400), yellow ligament (f: original magnification: ×400) and spinal cord (g: original magnification: ×400). Arrows in each figure point to strong staining of bone marrow cells (b), moderate staining of chondrocytes and hyaline cartilage cells (c), fibrous cells (d–f) and neurons (g).

Intervertebral discs act as 'shock absorbers' and joints during activity, allowing the spine to move freely. They consist of an outer fibrous ring and an inner nucleus pulposus. The discs are avascular, with sparsely distributed chondrocytes. It has been reported that BMPRs are present in cervical intervertebral discs in senescence-accelerated mice and in anterior margin cells in the cervical discs of a mouse spondylosis model.[11,12] In the current study, BMPR-1a was not stained in intervertebral discs, and BMP-2, BMPR-1b, -2, and Noggin were equally stained in chondrocytes, hyaline cartilage cells and fibrous cells in the cervical, thoracic and lumbar intervertebral discs. The relative distribution of BMP-2, BMPR-1b, -2 and Noggin in cervical, thoracic and lumbar intervertebral discs suggests that there is a relationship between their development and the BMP signaling pathway.

Bone marrow cells include pluripotent mesenchymal cells that are thought aid repair or maintain cells in other tissues, and produce various cytokines such as BMPs.[8] In this report, the expression of BMP-2, BMPR-1b, Noggin and particularly the strong expression of BMPR-1b in bone marrow cells, points to BMP signaling in bone marrow.

Recent studies have clearly demonstrated that BMP gene therapy with adenoviral vectors or rhBMP-2 implantation is useful for the induction of spinal arthrodesis or bone healing and regeneration in several animal models.[20] However, these studies have not provided sufficient data to warrant clinical application at this point.[21] There have been no reports using BMPRs or Noggin gene therapies in vivo in humans thus far. In this study, the expression of BMPR-1a or -1b in the yellow ligament, and Noggin in the anterior longitudinal, posterior longitudinal and yellow ligaments was detected by in situ hybridization. Understanding of the expression and action of these molecules may lead to the design of a gene therapy approach for the treatment of ligamentous ossification. However, further preclinical and clinical research and development are required before this technology will have direct clinical utility.

## References


1. Miyazono K, Ichijo H, Heldin CH. Transforming growth factor-beta: latent forms, binding proteins and receptors. *Growth Factors* 1993;**8**:11–22.
2. Fujii M, Takeda K, Imamura T, et al. Roles of bone morphogenetic protein type I receptors and Smad proteins in osteoblast and chondroblast differentiation. *Mol Biol Cell* 1999;**10**:3801–13.
3. Ishidou Y, Kitajima I, Obama H, et al. Enhanced expression of type I receptors for bone morphogenetic proteins during bone formation. *J Bone Miner Res* 1995;**10**:1651–9.
4. Kaneko H, Arakawa T, Mano H, et al. Direct stimulation of osteoclastic bone resorption by bone morphogenetic protein (BMP)-2 and expression of BMP receptors in mature osteoclasts. *Bone* 2000;**27**:479–86.
5. Onishi T, Ishidou Y, Nagamine T, et al. Distinct and overlapping patterns of localization of bone morphogenetic protein (BMP) family members and a BMP type II receptor during fracture healing in rats. *Bone* 1998;**22**:605–12.
6. Gazzerro E, Gangji V, Canalis E. Bone morphogenetic proteins induce the expression of noggin, which limits their activity in cultured rat osteoblasts. *J Clin Invest* 1998;**102**:2106–14.
7. Holley SA, Neul JL, Attisano L, et al. The Xenopus dorsalizing factor noggin ventralizes Drosophila embryos by preventing DPP from activating its receptor. *Cell* 1996;**86**:607–17.
8. Shimakura Y, Yamazaki Y, Uchinuma E. Experimental study on bone formation potential of cryopreserved human bone marrow mesenchymal cell/hydroxyapatite complex in the presence of recombinant human bone morphogenetic protein-2. *J Craniofac Surg* 2003;**14**:108–16.
9. Zimmerman LB, De Jesus-Escobar JM, Harland RM. The Spemann organizer signal noggin binds and inactivates bone morphogenetic protein 4. *Cell* 1996;**86**:599–606.
10. Yonemori K, Imamura T, Ishidou Y, et al. Bone morphogenetic protein receptors and activin receptors are highly expressed in ossified ligament tissues of patients with ossification of the posterior longitudinal ligament. *Am J Pathol* 1997;**150**:1335–47.
11. Nakase T, Ariga K, Miyamoto S, et al. Distribution of genes for bone morphogenetic protein-4, -6, growth differentiation factor-5, and bone morphogenetic protein receptors in the process of experimental spondylosis in mice. *J Neurosurg* 2001;**94**(1 Suppl):68–75.
12. Takae R, Matsunaga S, Origuchi N, et al. Immunolocalization of bone morphogenetic protein and its receptors in degeneration of intervertebral disc. *Spine* 1999;**24**:1397–401.
13. Zhao M, Harris SE, Horn D, et al. Bone morphogenetic protein receptor signaling is necessary for normal murine postnatal bone formation. *J Cell Biol* 2002;**157**:1049–60.
14. Yoshimura Y, Nomura S, Kawasaki S, Tsutsumimoto T, Shimizu T, Takaoka K. Colocalization of noggin and bone morphogenetic protein-4 during fracture healing. *J Bone Miner Res* 2001;**16**:876–84.
15. Nakamura Y, Wakitani S, Nakayama J, Wakabayashi S, Horiuchi H, Takaoka K. Temporal and spatial expression profiles of BMP receptors and Noggin during BMP-2 induced ectopic bone formation. *J Bone Miner Res* 2003;**18**:1854–62.
16. Lein PJ, Beck HN, Chandrasekaran V, et al. Glia induce dendritic growth in cultured sympathetic neurons by modulating the balance between bone morphogenetic proteins (BMPs) and BMP antagonists. *J Neurosci* 2002;**22**:10377–87.
17. Lim DA, Tramontin AD, Trevejo JM, Herrera DG, Garcia-Verdugo A, Alvarez-Buylla A. Noggin antagonizes BMP signaling to create a niche for adult neurogenesis. *Neuron* 2000;**28**:713–26.
18. Gomes WA, Mehler MF, Kessler JA. Transgenic overexpression of BMP4 increases astroglial and decreases oligodendroglial lineage commitment. *Dev Biol* 2003;**255**:164–77.
19. Mekki-Dauriac S, Agius E, Kan P, Cochard P. Bone morphogenetic proteins negatively control oligodendrocyte precursor specification in the chick spinal cord. *Development* 2002;**129**:5117–30.
20. Nishida K, Kang JD, Gilbertson LG, et al. Modulation of the biologic activity of the rabbit intervertebral disc by gene therapy: an in vivo study of adenovirus-mediated transfer of the human transforming growth factor beta 1 encoding gene. *Spine* 1999;**24**:2419–25.
21. Takahashi J, Saito N, Ebara S, et al. Anterior thoracic spinal fusion in dogs by injection of recombinant human bone morphogenetic protein-2 and a synthetic polymer. *J Spinal Disord* 2003;**16**:137–43.

Volume 54(12): 1371–1378, 2006
Journal of Histochemistry & Cytochemistry
http://www.jhc.org

ARTICLE

# Immunohistochemical Localization of α-Smooth Muscle Actin During Rat Molar Tooth Development

Akihiro Hosoya, Hiroaki Nakamura, Tadashi Ninomiya, Kunihiko Yoshiba, Nagako Yoshiba, Hiroyuki Nakaya, Shigeyuki Wakitani, Hirohito Yamada, Etsuo Kasahara, and Hidehiro Ozawa

Department of Oral Histology (AH,HNakamura), Institute for Dental Science (TN,HO), and Department of Endodontics and Operative Dentistry (HY,EK), Matsumoto Dental University, Shiojiri, Nagano, Japan; Division of Cariology, Department of Oral Health Science, Course for Oral Life Science, Niigata University Graduate School of Medical and Dental Sciences, Niigata, Japan (KY,NY); and Department of Orthopedic Surgery, Shinshu University Graduate School of Medicine, Matsumoto, Nagano, Japan (HNakaya,SW)

SUMMARY The dental follicle contains mesenchymal cells that differentiate into osteoblasts, cementoblasts, and fibroblasts. However, the characteristics of these mesenchymal cells are still unknown. α-Smooth muscle actin (α-SMA) is known to localize in stem cells and precursor cells of various tissues. In the present study, to characterize the undifferentiated cells in the dental follicle, immunohistochemical localization of α-SMA was examined during rat molar tooth development. Rat mandibles were collected at embryonic days (E) 15–20 and postnatal days (P) 7–28. Immunohistochemical stainings for α-SMA, periostin, Runt-related transcription factor-2 (Runx2), tissue nonspecific alkaline phosphatase (TNAP), and bone sialoprotein (BSP) were carried out using paraffin-embedded sections. α-SMA localization was hardly detected in the bud and cap stages. At the early bell stage, α-SMA-positive cells were visible in the dental follicle around the cervical loop. At the late bell to early root formation stage (P14), these cells were detected throughout the dental follicle, but they were confined to the apical root area at P28. Double immunostaining for α-SMA and periostin demonstrated that α-SMA-positive cells localized to the outer side of periostin-positive area. Runx2-positive cells were visible in the α-SMA-positive region. TNAP-positive cells in the dental follicle localized nearer to alveolar bone than Runx2-positive cells. BSP was detected in osteoblasts as well as in alveolar bone matrix. These results demonstrate that α-SMA-positive cells localize on the alveolar bone side of the dental follicle and may play a role in alveolar bone formation.
(J Histochem Cytochem 54:1371–1378, 2006)

KEY WORDS
α-smooth muscle actin
dental follicle
undifferentiated cell
rat molar
periostin

THE DENTAL FOLLICLE surrounding the tooth germ contains mesenchymal cells that are able to differentiate into osteoblasts, cementoblasts, and fibroblasts (Nanci 2003). As a result, this tissue is able to form the periodontal tissues including alveolar bone, cementum, and periodontal ligament. However, the characteristics and distribution of undifferentiated cells within the dental follicle and periodontal tissues are still unclear.

Previous reports have described α-smooth muscle actin (α-SMA) as a cytoskeletal protein that is localized to some stem and precursor cells (Cai et al. 2001; Kinner et al. 2002; Yamada et al. 2005). This protein has also been found in various tissues during tissue repair and regeneration following injury (Chaponnier and Gabbiani 2004; van Beurden et al. 2005). Thus, α-SMA may be a suitable marker of undifferentiated cells (Kinner et al. 2002). Additionally, in mature tissues, α-SMA is localized to pericytes of blood vessels, intestinal muscularis mucosae, and myoepithelial cells of mammary and salivary glands (Mukai et al. 1981; Skalli et al. 1986), which are required in a force-generating capacity. However, the temporospatial localization of α-SMA in developing and mature teeth has not been previously examined.

On the other hand, regeneration of periodontal tissues, lost as a result of periodontal disease, is a key

Correspondence to: Akihiro Hosoya, DDS, PhD, Department of Oral Histology, Matsumoto Dental University, 1780 Gobara Hirooka, Shiojiri, Nagano 399-0781, Japan. E-mail: hosoya@po.mdu.ac.jp

Received for publication March 29, 2006; accepted July 21, 2006 [DOI: 10.1369/jhc.6A6980.2006].



0022-1554/06/$3.30

objective of periodontal treatment. Several surgical techniques have been developed to assist with regeneration of periodontal tissues including guided tissue regeneration, bone grafting, and the use of enamel matrix derivative (Emdogain; Straumann, Basel, Switzerland), but their success is not predictable. Development of new periodontal regeneration therapies using the undifferentiated cells in the periodontal tissues thus remains ongoing. The human periodontal ligament contains multipotent stem cells that differentiate into osteoblasts, cementoblasts, and fibroblasts, and these cells could possibly be used to induce periodontal regeneration (Seo et al. 2004,2005). Additionally, the dental follicle has been utilized as a source of undifferentiated cells in in vitro and in vivo studies (Saito et al. 2005). Because the dental follicle and periodontal ligament are immunopositive for periostin (Kruzynska-Frejtag et al. 2004; Suzuki et al. 2004), this protein is often used as a marker of these tissues. However, determining the degree of cell differentiation could not be readily ascertained. A more definitive understanding of the periodontal tissue could assist with the development of regenerative methods using periodontal cells.

The differentiation process of alveolar bone-formative osteoblasts has also not been clarified. Bone morphogenetic proteins (BMPs) and/or transforming growth factor (TGF)-β act on undifferentiated cells and phosphorylate R-Smads through their receptors. These phosphorylated R-Smads subsequently interact with Smad4 and translocate to the nucleus (Derynck et al. 1998; Shi and Massague 2003). Thereafter, Runx2, the essential transcription factor for osteoblast differentiation, is expressed in osteogenic cells and induces the expression of bone matrix proteins such as osteopontin (OPN) and bone sialoprotein (BSP) (Lian et al. 2004). In these processes, expression of tissue nonspecific alkaline phosphatase (TNAP) is also increased (Hoshi et al. 1997; Hosoya et al. 2003).

In the present study, we show that α-SMA is specifically expressed in the dental follicle. In addition, to examine the distribution pattern of α-SMA and the differentiation process of these positive cells, immunohistochemical localization of α-SMA and other differentiation marker proteins were examined during rat molar tooth development. The marker of the dental follicle used was periostin-specific antibody. Observations of cell differentiation process in α-SMA-positive area were also undertaken and involved the use of Smad4-, Runx2-, OPN-, BSP-, and TNAP-specific antibodies.

## Materials and Methods

All experiments were performed according to guidelines set forth by the Matsumoto Dental University Committee on Intramural Animal Use.

### Western Blotting

First molar tooth germs of E15, 17, and 20 Wistar rats were removed from the mandible. Samples were dissolved in 100 μl of sample buffer containing 4% SDS, 20% glycerol, and 12% mercaptoethanol in 100 mM Tris–HCl (pH 6.8) and heated at 100C for 5 min. These lysates were quantified by BCA protein assay kit (Pierce Biotechnology; Rockford, IL), and an equal amount (30 μg) of each lysate was fractionated by SDS-PAGE using 12% polyacrylamide gel. Samples were then electrophoresed at 150 V for 60 min and transferred to a nitrocellulose membrane using 192 mM glycine and 20% methanol in 25 mM Tris–HCl (pH 8.3) at a constant amperage of 50 mA for 60 min. The membrane was immersed in 10 mM TBS, pH 7.4, containing 10% skim milk for 30 min to block nonspecific binding. It was subsequently incubated with mouse monoclonal antibody against human α-SMA (1A4;R&D Systems, Minneapolis, MN), diluted 1:1000 for 12 hr at 4C, and then with horseradish peroxidase (HRP)-conjugated anti-mouse IgG (Sigma; St Louis, MO) for 1 hr at room temperature. Immunoreactivity was visualized using ECL Western blotting detection reagents (Amersham Pharmacia Biotech UK Ltd.; Buckinghamshire, England) according to the manufacturer's instructions. The membrane was then reprobed in 2% SDS, 62.5 mM Tris–HCl (pH 6.7), and 100 mM 2-mercaptoethanol for 30 min at 50C and subsequently incubated with rabbit anti-mouse actin polyclonal antibody (Biomedical Technologies; Stoughton, MA), and HRP-conjugated anti-rabbit IgG (Sigma) for comparison of the amount of total protein.

### Immunohistochemistry

Rat mandibles were collected at E15–20 and P7–28 and fixed with 4% paraformaldehyde in 0.1 M phosphate buffer (pH 7.4) for 24 hr at 4C. After demineralization with 10% EDTA, pH 7.4, for 3 weeks at 4C, the specimens were embedded in paraffin and sectioned at a thickness of 4 μm. Sections were then treated with 0.3% $H_2O_2$ in PBS, pH 7.4, for 30 min at room temperature to inactivate endogenous peroxidase. They were pretreated with 10% BSA (Seikagaku; Tokyo, Japan) in PBS for 1 hr at room temperature and incubated in mouse monoclonal antibodies against human α-SMA, human Smad4 (Santa Cruz Biotechnology; Santa Cruz, CA), and rabbit polyclonal antibodies against mouse Runx2 (Santa Cruz Biotechnology), rat TNAP (provided by Dr. Y. Ikehara), mouse OPN (provided by Dr. M. Fukae), human BSP (LF-120, provided by Dr. L.W. Fisher) for 12 hr at 4C. The antibodies against α-SMA, TNAP, OPN, and BSP were diluted to 1:500, and Smad4 and Runx2 antibodies were diluted to 1:100. Sections were reacted with Histofine Simple Stain rat MAX-PO (MULTI; Nichirei Co., Tokyo, Japan) for 1 hr at room temperature. Immune complexes were visualized using DAB (Envision kit; DAKO, Carpinteria, CA). Immunostained sections were then counterstained with hematoxylin. Non-immune mouse or rabbit sera were diluted to the same strength for use as negative controls. Control sections did not show any specific immunoreactivity.

Double-immunofluorescence staining was performed using mouse monoclonal antibody against human α-SMA and rabbit polyclonal antibody against human periostin (Bio-Vendor Laboratory; Heidelberg, Germany). Sections were pretreated with 10% BSA in PBS for 1 hr at room temperature

and incubated with 1:100 diluted primary antibodies for 12 hr at 4C. Sections were then incubated with 1:100 diluted Alexa-Fluor-488-conjugated anti-mouse IgG (Molecular Probes; Eugene, OR) and Alexa-Fluor-594-conjugated anti rabbit IgG (Molecular Probes) as secondary antibodies for 1 hr at room temperature. Samples were evaluated using a fluorescent microscope (Axioplan 2; Carl Zeiss, Jena, Germany) with the appropriate filter combinations.

## Results

### Localization of α-SMA During the Bud, Cap, and Early Bell Stages of Tooth Development

Western blotting analysis revealed that α-SMA antibody did not react with the lysate of E15 mandibular molar tooth germ. However, this antibody did react with the lysate of E17 and E20 tooth germs, with the intensity of reactivity increasing as tooth development progressed (Figure 1A).

Immunohistochemical localization of α-SMA was scarce in the tooth germ at the bud (E15) and cap (E17) stages (Figures 1B and 1C). At the early bell stage (E20), the dental follicle around the cervical loop displayed α-SMA immunoreactivity (Figures 1D and 1E). This immunoreactivity was seen within the cytoplasm of dental follicle cells possessing long cell processes (Figure 1F). The enamel organ and dental papillae showed no immunoreactivity.

### Localization of α-SMA During the Late Bell and Root Formation Stages of Tooth Development

At the late bell stage (P7), α-SMA-positive cells were seen in the dental follicle surrounding the enamel organ

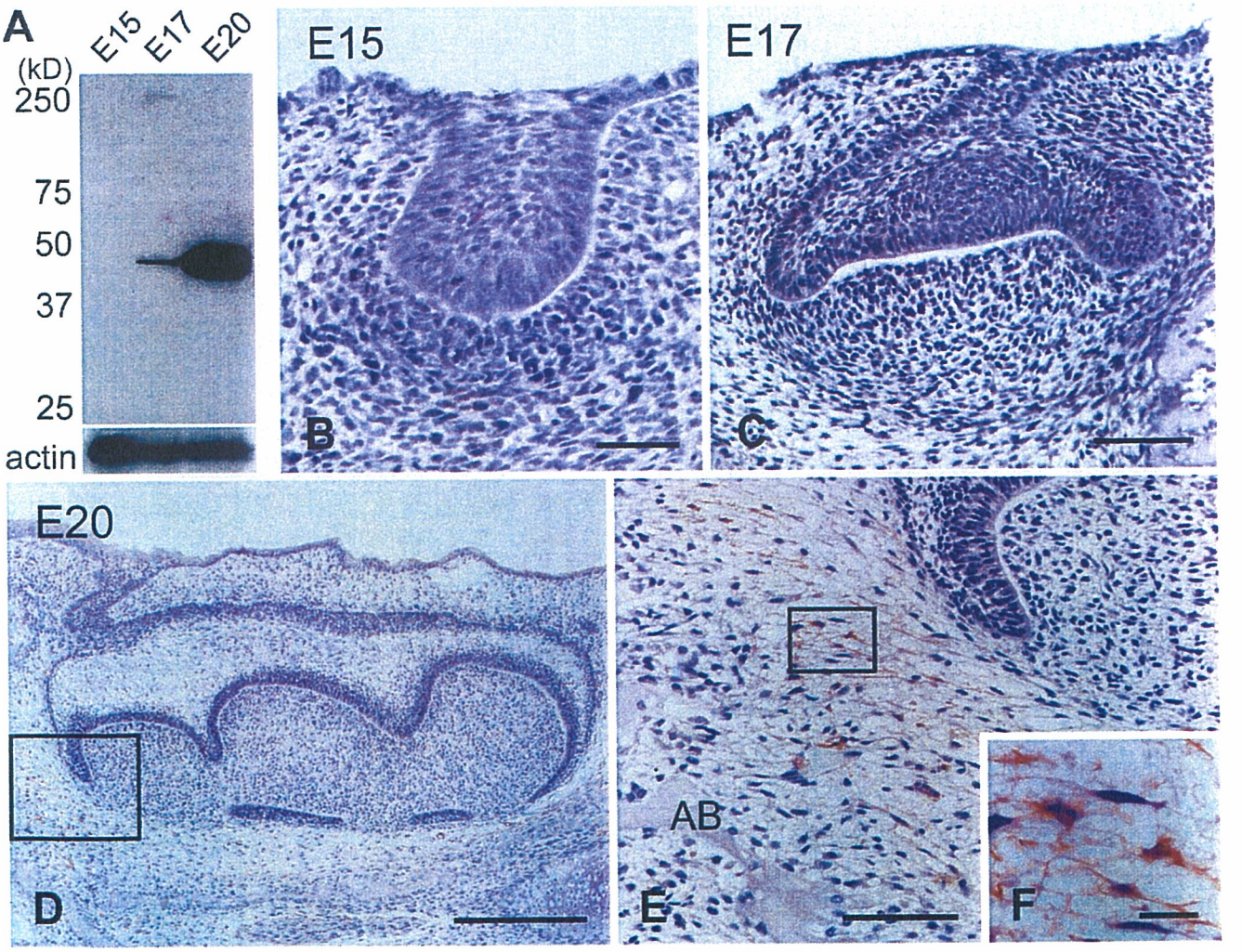


**Figure 1** Western blotting analysis (A) and immunohistochemical staining of α-smooth muscle actin (αSMA) in the mandibular first molar at E15 (B), E17 (C), and E20 (D–F). Higher magnification of the boxed regions in D and E are shown in E and F, respectively. (A) α-SMA antibody reacted with cells in the E17 and E20 tooth germ. (B,C) α-SMA-positive cells are scarce in the tooth germs at the bud and cap stages. (D,E) The dental follicle cells around the cervical loop show α-SMA immunoreactivity at the early bell stage. (F) These cells exhibit long cell processes. AB, alveolar bone. Bars: B,E = 60 μm; C = 100 μm; D = 300 μm; F = 10 μm.

(Figure 2A). These cells seemed to localize on the alveolar bone side of the dental follicle (Figures 2B and 2C). Pericytes and smooth muscle cells of blood vessels surrounding the tooth germ and within the bone marrow displayed immunoreactivity. The surface of the alveolar bone, except the surface adjacent to the tooth germ, showed no immunoreactivity (Figure 2A). At the root formation stage (P14), intense immunostaining for α-SMA was observed in the dental follicle around Hertwig's epithelial root sheath (HRS). The dental follicle surrounding the enamel organ showed weaker immunoreactivity than that around HRS (Figures 2D–2F). As root formation progressed (P28), α-SMA-positive cells were confined to the apical region of the dental follicle (Figures 3A and 3C). In the upper region of the periodontal space, there was no immunoreactivity for α-SMA, except for that associated with the blood vessels (Figure 3B). In the pulp tissue, pericytes and smooth muscle cells of the blood vessels were positive for α-SMA, but odontoblasts and pulp cells showed no immunoreactivity (Figure 3A).

### α-SMA and Periostin Localization in the Dental Follicle

In the root apex of P28, α-SMA-positive cells were localized to the dental follicle. Pericytes and smooth muscle cells of the blood vessels in the periodontal space were also immunopositive for α-SMA (Figure 4A). Periostin was localized to the apical region of the dental follicle and

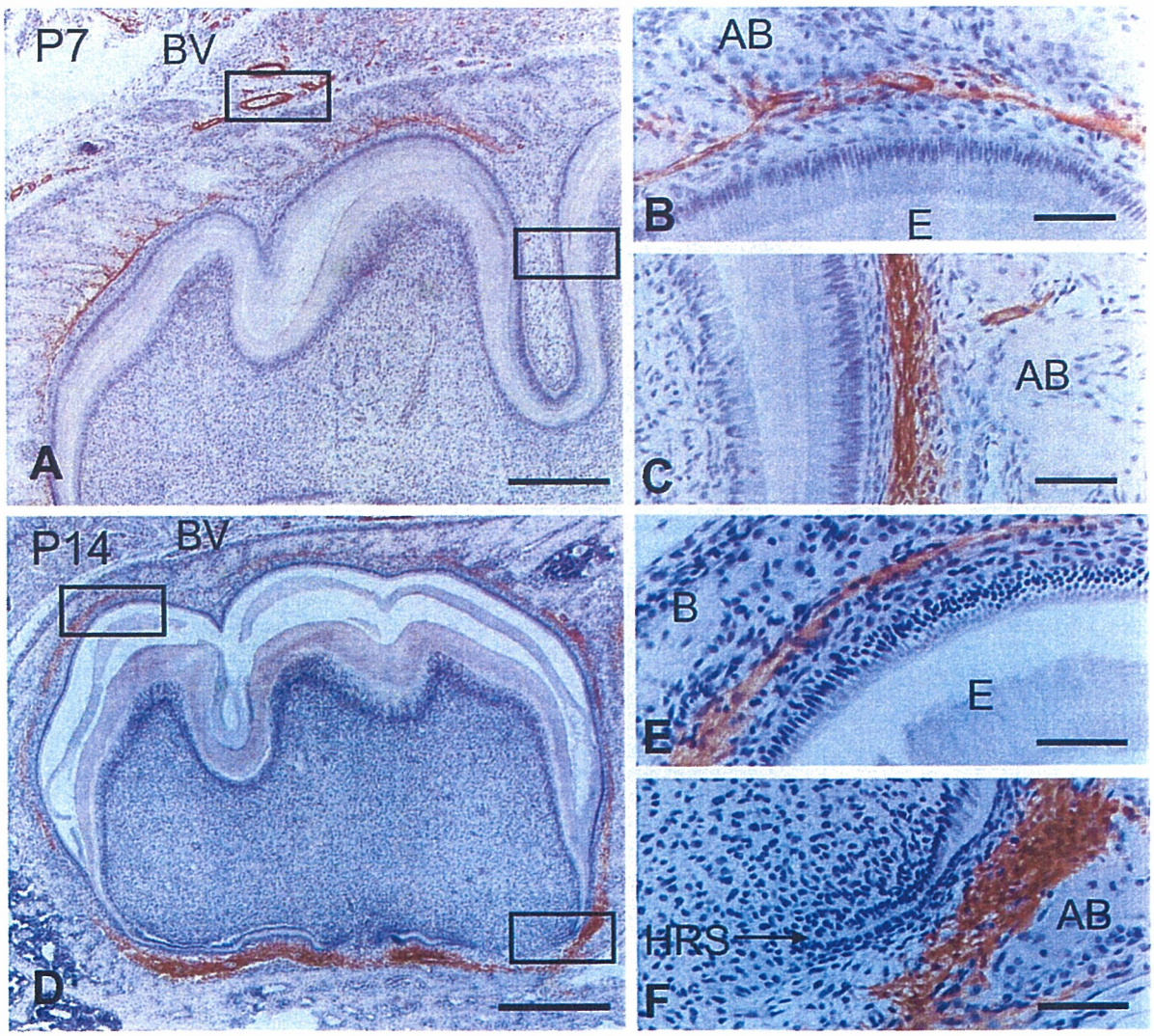


**Figure 2** Immunohistochemical staining of α-SMA in the mandibular first molar at P7 (**A–C**) and P14 (**D–F**). Higher magnification of the boxed regions in **A** and **D** are shown in **B** and **C** and **E** and **F**, respectively. (**A**) α-SMA immunoreactivity is localized to the dental follicle surrounding the tooth crown at the late bell stage. (**B,C**) α-SMA-positive cells are visible on the alveolar bone (AB) side of the dental follicle. (**D–F**) Intense immunostaining for α-SMA is detected in the dental follicle along Hertwig's epithelial root sheath (HRS), whereas the dental follicle surrounding the tooth crown shows less immunoreactivity. BV, blood vessel; E, enamel. Bars: **A,D** = 600 μm; **B,C,E,F** = 100 μm.